NBS SPECIAL PUBLICATION 260-59

U.S. DEPARTMENT OF COMMERCE / National Bureau of Standards

Standard Reference Materials:

ELECTRON PARAMAGNETIC RESONANCE INTENSITY STANDARD: SRM-2601; DESCRIPTION AND USE

Standard Reference Materials:

ELECTRON PARAMAGNETIC RESONANCE INTENSITY STANDARD: SRM 2601; DESCRIPTION AND USE

T. Chang
A.H. Kahn

Center for Materials Science
National Measurement Laboratory
National Bureau of Standards
Washington, D.C. 20234

U.S. DEPARTMENT OF COMMERCE, Juanita M. Kreps, Secretary

Dr. Sidney Harman, Under Secretary

Jordan J. Baruch, Assistant Secretary for Science and Technology

NATIONAL BUREAU OF STANDARDS, Ernest Ambler, Director

Issued August 1978

Library of Congress Catalog Card Number 78-600064

National Bureau of Standards Special Publication 260-59
Nat. Bur. Stand. (U.S.), Spec. Publ. 260-59, 60 pages (Aug. 1978)
CODEN: XNBSAV

U.S. GOVERNMENT PRINTING OFFICE
WASHINGTON: 1978

For sale by the Superintendent of Documents, U.S. Government Printing Office, Washington, D.C. 20402
Stock No. 003-003-01975-5 Price $2.30
(Add 25 percent additional for other than U.S. mailing).

PREFACE

Standard Reference Materials (SRM's) as defined by the National Bureau of Standards are "well-characterized materials, produced in quantity, that calibrate a measurement system to assure compatibility of measurement in the nation." SRM's are widely used as primary standards in many diverse fields in science, industry, and technology, both within the United States and throughout the world. In many industries traceability of their quality control process to the national measurement system is carried out through the mechanism and use of SRM's. For many of the nation's scientists and technologists it is therefore of more than passing interest to know the details of the measurements made at NBS in arriving at the certified values of the SRM's produced. An NBS series of papers, of which this publication is a member, called the NBS Special Publication - 260 Series is reserved for this purpose.

This 260 Series is dedicated to the dissemination of information on all phases of the preparation, measurement, and certification of NBS-SRM's. In general, much more detail will be found in these papers than is generally allowed, or desirable, in scientific journal articles. This enables the user to assess the validity and accuracy of the measurement processes employed, to judge the statistical analysis, and to learn details of techniques and methods utilized for work entailing the greatest care and accuracy. It is also hoped that these papers will provide sufficient additional information not found on the certificate so that new applications in diverse fields not foreseen at the time the SRM was originally issued will be sought and found.

Inquiries concerning the technical content of this paper should be directed to the author(s). Other questions concerned with the availability, delivery, price, and so forth will receive prompt attention from:

Office of Standard Reference Materials
National Bureau of Standards
Washington, D.C. 20234

J. Paul Cali, Chief
Office of Standard Reference Materials

Contents Page

List of Tables

List of Figures

Standard Reference Materials:

ELECTRON PARAMAGNETIC RESONANCE INTENSITY STANDARD: SRM-2601;

Description and Use.

T. Chang and A. H. Kahn

Ceramics, Glass, and Solid State Science Division
Center for Materials Science
National Measurement Laboratory
National Bureau of Standards
Washington, D. C. 20234

Abstract

This publication provides information concerning the use of ruby samples, of known Cr^{3+} concentration, supplied as a Standard Reference Material (SRM) for intensity measurements in electron paramagnetic resonance (EPR) experiments. By comparing the measured intensities of EPR absorption lines of a test sample and of the SRM, it is often possible for the user to obtain a determination of the number of spins in the test sample. Procedures and data on ruby necessary for carrying out this process are presented. Examples of the use of the SRM in typical cases are offered.

Keywords: Absolute measurement; intensity standard; paramagnetic resonance; spin concentration; Standard Reference Material (SRM); ruby

1. Introduction

This instruction manual is supplied as an aid in using the NBS Electron Paramagnetic Resonance (EPR) Intensity Standard Reference Material (SRM). It provides suggestions for use of the SRM for measuring the number of active paramagnetic centers in a test sample. This measurement is performed by comparison of the area of the test EPR absorption line with that of an EPR absorption line of the ruby SRM. This method is satisfactory if the test resonance is reasonably narrow (about 100 Oe or less) and is describable by a spin Hamiltonian. Even if the test spectrum is not well understood, comparisons of resonance line areas can be used to obtain relative measurements of the number of spins in test samples.

The nature of the EPR experiment is outlined so that the nomenclature and symbols used may be defined unambiguously. For a more detailed description, the user is referred to any standard text [1-6]. For further details concerning the spectrum of ruby and the research leading to the preparation of the Ruby SRM, the user is referred to a publication by the authors [7].

In the conventional EPR measurement, the sample to be tested is placed in a sample cavity at a site of uniform microwave magnetic field, H_1. The cavity is located in a uniform static field, H_o, at right angles to H_1. The field H_o is modulated at a low frequency (typically 30 Hz to 200 kHz) for signal detection. The static field is slowly varied until the spins in the sample satisfy the resonance condition, that the difference of energy, ΔE, of two of their energy levels in the magnetic field, coincides with the microwave radiation according to the relation,

$$\Delta E = h\nu, \tag{1}$$

where h is Planck's constant and ν is the microwave frequency. A recording of the change of cavity power dissipation, induced by the spins going into resonance as H_o is varied, is referred to as the EPR absorption curve. The usual experimental arrangement produces a recording of the derivative with respect to H_o of the absorption curve, and one integration is necessary to obtain the absorption curve. A further integration with respect to H_o yields the area under the absorption curve (see section 5.1). This area is the measure of the intensity of the particular resonance absorption being studied. The EPR spectrometer, as commonly used, gives the data in arbitrary units. By comparing the absorption signal of the test sample with the signal from a standard sample having a known number of spins and a well-understood spectrum, it is possible, in many cases, to determine the number of the unknown spins.

The area under the absorption curve of an EPR line can be written as a product of four factors, as follows:

---

* Numbers in brackets refer to literature references at the end of the paper.

Area = [Spectrometer gain factor] x [Filling factor]
x [Concentration of spins]
x [Integrated intensity per spin in unit RF field] (2)

a) The first factor depends on spectrometer conditions. This factor will include detection efficiency, demodulation efficiency, amplifier gain, etc. When comparing two different resonances, it is desirable to hold this factor constant.

b) The second factor is the filling factor, defined by

$$\eta = \frac{\langle H_1^2 \rangle_s V_s}{\langle H_1^2 \rangle_c V_c} \tag{3}$$

where V_s is the sample volume, V_c the cavity volume, and the brackets indicate the average of H_1^2 over the sample(s) or cavity (c). This factor accounts for the fact that the absorption intensity is proportional to the square of the microwave field amplitude acting on the spins. Filling factors are tabulated in reference [3].

c) The third factor corresponds to the fact that the absorption per unit volume of the sample is proportional to the concentration of spins.

d) The last factor is the absorption per single spin, per unit microwave field amplitude. This factor depends in detail on the nature of the absorbing center, its spin, energy levels, and the direction of applied fields. This factor has been computed for Cr^{3+} in ruby [7] for a wide range of conditions and the results are available from tables supplied in this manual.

On performing a slight rearrangement of the second and third factors, we obtain the form,

$$\text{Area} = [\text{Spectrometer gain factor}] \times \frac{\langle H_1^2 \rangle_s}{\langle H_1^2 \rangle_c} \frac{1}{V_c}$$

x [Total number of spins]
x [Integrated intensity per spin] (4)

which explicitly demonstrates that the area is proportional to the number of spins in the sample.

The area under the EPR absorption curve must be used for the measurement of the number of spins. The product of the square of the linewidth and the peak-to-peak height is an approximation to the area and may not give an accurate value. It is important that the user have available the facility for performing the double integrations numerically, either by computer or by graphical methods; otherwise, the measurement of the number of spins can not be accomplished.

The EPR standard sample made of ruby is one of the Standard Reference Materials (SRM's) certified and issued by the National Bureau of Standards. Hence, we shall call the standard sample the EPR SRM. Wherever we mention the SRM in this publication, we mean the EPR SRM only and do not refer to any other types of SRM's. We use the terms standard samples, ruby standards, ruby specimen, or simply SRM, interchangeably.

2. Theory

2.1 Ruby Crystal

The EPR SRM specimens were cut from single crystal ruby, i.e., chromium (Cr) doped corundum (Al_2O_3). These crystals possess trigonal symmetry. The trigonal axis is a unique axis of the crystal and is called the c-axis.

The chromium ions in ruby are substitutional for the aluminum ions, and assume the trivalent state Cr^{3+}. They are the active ingredient which provides the EPR absorption centers. The Cr^{3+} ions experience the same crystalline environment as the aluminum ions. As a consequence of the crystalline symmetry and the properties of the Cr^{3+} ions, the EPR spectrum of the Cr^{3+} in ruby is strongly dependent on the angle, θ, between the static field, H_o, and the c-axis. The spectrum does not vary when the static field, H_o, is rotated in a plane which is normal to the c-axis.

In the next two sections, we give a brief description of the energy levels of the Cr^{3+} ion in ruby. Formulas are presented for completeness, but the user can obtain all needed information from the tables, as explained in section 2.5.

2.2 The Cr^{3+} Spectrum with H_o Parallel to the c-axis

The EPR spectrum for H_o parallel to the c-axis, i.e., $\theta = 0°$, is the simplest. In this case the energy levels of the Cr^{3+} ions of concern in the EPR experiment are given by the expression

$$E_m = g_{\parallel} \mu_B H_o m + D\,(m^2 - 5/4), \tag{5}$$

where μ_B is the Bohr magneton, H_o is the static field, $g_\parallel$ is the parallel g-factor, D is the zero field splitting factor, and m is the magnetic quantum number. Cr^{3+} has spin 3/2 and thus m can assume any of the four values of 3/2, 1/2, -1/2, and -3/2. Whenever the applied microwave frequency satisfies the relation

$$h\nu = \Delta E = E_{m+1} - E_m = g_\parallel \mu_B H_o + (2m+1)D \quad , \tag{6}$$

resonance absorption can occur. We may denote the transition by pairs of indices (m+1,m), i.e., (3/2,1/2), (1/2,-1/2), and (-1/2,-3/2). There are three allowed transitions.

2.3 The Cr^{3+} Spectrum with H_o Not Parallel to the c-axis

When the c-axis and the static magnetic field are not parallel, there are still four energy levels for Cr^{3+} ions, but they can not be described in the simple form of Eq. (5); also, another parameter $g_\perp$, the perpendicular g-factor, is needed. In this case, the energy states may not be described by the simple quantum numbers m; we choose to label the levels by the numbers 1,2,3,4 from the highest energy in sequence downward. In general, there are six possible distinct transitions and we label them (1,2), (1,3), etc. A particular transition in this notation is referred to by the symbol (α,β). Not all transitions will be strong enough to be observed.

When the field H_o is parallel to the c-axis, we may use either the labelling method of this section or of the previous section.

From our measurements, the values of the constants for Cr^{3+} in ruby are

$$\begin{aligned} g_\parallel &= 1.9817 \pm 0.0004 \\ g_\perp &= 1.9819 \pm 0.0006 \\ 2D/h &= -11.493 \pm 0.004 \text{ GHz} \quad . \end{aligned} \tag{7}$$

2.4 Polarization of the Microwave Field and the Integrated Intensity

The values of the resonance fields for a given microwave frequency depend on the angle between H_o and the c-axis of the ruby crystal. However, the intensity of a particular resonance line further depends on the direction of the RF field, H_1, i.e., on its direction of polarization. (We remember that H_1 is always perpendicular to the static field, H_o.)

To specify the orientation of the various field vectors with respect to the crystalline c-axis of the ruby SRM, we introduce a set of mutually perpendicular reference axes x', y', and z', which will be called the laboratory coordinate system. The z'-axis is chosen to lie along the direction of the static field, H_o. The x'-axis, perpendicular

to H_o, is selected to lie in the plane of the crystalline c-axis and the z'-axis. (If the c-axis is parallel to the z'-axis, the direction of the x'-axis will be arbitrary.) Lastly, the y'-axis is chosen normal to the x'- and z'-axes. EPR experiments are usually performed with the RF field, H_1, parallel to the x'- or y'- axes. In these cases we refer to the RF field as having x'- or y'- polarization, respectively. The two polarizations will induce the same EPR transitions at a given static field, H_o, but the line intensities will be different. Information concerning the polarizations for particular cavities and crystal mounting will be given in Sec. 4.3.

The integrated intensity associated with a single Cr^{3+} ion is theoretically determined if the particular transition and direction of polarization are specified. The intensity has been calculated from the transition probability rate according to the usual theory of the intensity of spectral lines [7]. This theory gives the result that one would obtain if line profiles were obtained by sweeping frequency. The areas would be proportional to the transition probability rates $T_{x'}$ or $T_{y'}$, for the polarizations x' or y'. However, in the usual EPR experiment the absorption line profile is obtained by sweeping the field H_o. In this, the common case, the integrated intensity (per spin) can be obtained from the transition probabilities divided by a weighting factor, $d\nu_{\alpha\beta}/dH_o$, the rate of change of resonance frequency with respect to H_o for the (α,β) transition. The field-sweep integrated intensity will be denoted by $U_{x'}$ or $U_{y'}$.

The transition probabilities, $T_{x'}$, $T_{y'}$, are normalized so that the quantities at (1/2,-1/2) are unity. The integrated intensities, $U_{x'}$, $U_{y'}$, are also normalized and adjusted so that the values for the (1/2,-1/2) transition are unity.

2.5 Tabulations and Graphs

The resonance fields, transition probabilities, and the integrated intensities are listed in Table 1 through Table 7. Each table corresponds to a commonly used microwave frequency. The frequencies are, respectively, 6.0, 9.5, 14.5, 18.0, 24.0, 35.0, and 50.0 GHz. In each table the EPR transitions are listed for values of θ, the angle between H_o and the c-axis, from 0° to 90° in steps of 10°.

In the tables the microwave frequency is identified in the caption. The resonances are grouped according to the value of θ, listed in column 1. Within the group for each angle, θ, the resonances are listed in order of increasing magnetic field, H_o. The resonance field values are listed in column 2. The units of magnetic fields are discussed in Appendix 1. The transitions are identified in column 3 according to the (α,β) notation (see Sec. 2.3). For $\theta = 0°$, the allowed transitions are also identified by the quantum numbers (m+1,m) (see Sec. 2.2). The normalized transition probabilities, $T_{x'}$, $T_{y'}$, are listed in columns 4 and 5. The integrated intensities, $U_{x'}$ and $U_{y'}$, are listed in columns 6 and 7.

Table 1. The resonance magnetic field, the transition probability, T, and the integrated intensity, U, of Cr^{3+} ion in ruby, for microwave frequency of 6.000 GHz.

ANGLE (Deg)	H (Oe)	TRANS.	$T_{x'}$	$T_{y'}$	$U_{x'}$	$U_{y'}$
0.0	721.1	(3,4)	.000	.000	.000	.000
	990.2	(2,3)	.000	.000	.000	.000
	1980.5	(1,3)($\frac{1}{2}$, $\frac{3}{2}$)	.750	.750	.750	.750
	2163.3	(1,3)($\frac{1}{2}$,$-\frac{1}{2}$)	1.000	1.000	1.000	1.000
	3153.5	(2,3)	.000	.000	.000	.000
	6306.6	(1,2)($\frac{3}{2}$,$\frac{1}{2}$)	.750	.750	.750	.750
10.0	732.6	(3,4)	.000	.000	.000	.000
	996.5	(2,3)	.035	.037	.018	.019
	2076.6	(1,2)	.162	1.630	.311	3.124
	2143.7	(1,2)	.051	1.441	.113	3.180
	3263.7	(2,3)	.261	.249	.149	.142
	5737.3	(1,2)	.501	.763	.608	.926
20.0	768.9	(3,4)	.000	.000	.000	.000
	1019.5	(2,3)	.096	.123	.051	.065
	1850.0	(1,2)	.458	1.235	.417	1.124
	3454.3	(2,3)	.539	.478	.362	.320
30.0	837.1	(3,4)	.001	.001	.000	.000
	1072.7	(2,3)	.120	.224	.071	.132
	1643.0	(1,2)	.407	1.159	.326	.930
	3545.3	(2,3)	.659	.582	.505	.446
40.0	952.3	(3,4)	.003	.003	.001	.001
	1178.1	(2,3)	.085	.325	.061	.233
	1473.0	(1,2)	.364	1.124	.265	.817
	3416.0	(2,3)	.615	.628	.565	.577
50.0	1150.4	(3,4)	.011	.012	.006	.007
	1343.7	(1,2)	.335	1.104	.225	.742
	1407.0	(2,3)	.015	.434	.017	.490
	2947.7	(2,3)	.392	.638	.530	.862
60.0	1250.4	(1,2)	.317	1.092	.200	.690
	1526.6	(3,4)	.050	.047	.040	.038
70.0	1187.9	(1,2)	.307	1.085	.186	.656
	2366.4	(3,4)	.290	.174	.372	.223
80.0	1151.6	(1,2)	.302	1.082	.178	.637
	3565.6	(3,4)	.935	.321	1.138	.391
90.0	1139.8	(1,2)	.300	1.081	.175	.630
	4048.4	(3,4)	1.262	.360	1.377	.393

Table 2. The resonance magnetic field, the transition probability, T, and the integrated intensity, U, of Cr^{3+} ion in ruby, for microwave frequency of 9.500 GHz.

ANGLE (Deg)	H (Oe)	TRANS.	$T_{x'}$	$T_{y'}$	$U_{x'}$	$U_{y'}$
0.0	359.4	(2,3)	.000	.000	.000	.000
	718.7	(1,3)($\frac{1}{2}$, $\frac{3}{2}$)	.750	.750	.750	.750
	1141.8	(3,4)	.000	.000	.000	.000
	3425.0	(1,3)($\frac{1}{2}$,$-\frac{1}{2}$)	1.000	1.000	1.000	1.000
	3784.4	(2,3)	.000	.000	.000	.000
	7568.8	(1,2)($\frac{3}{2}$,$\frac{1}{2}$)	.750	.750	.750	.750
10.0	360.2	(2,3)	.025	.026	.012	.013
	760.2	(1,3)	.688	.716	.737	.768
	1160.9	(3,4)	.000	.000	.000	.000
	3146.1	(1,3)	.793	.738	.645	.600
	4042.6	(2,3)	.541	.526	.368	.358
	7154.3	(1,2)	.646	.759	.692	.813
20.0	363.7	(2,3)	.074	.087	.038	.044
	920.3	(1,3)	.526	.622	.729	.861
	1221.9	(3,4)	.001	.001	.000	.000
	2730.5	(1,3)	.701	.397	.528	.299
	4351.6	(2,3)	.705	.656	.532	.495
	5948.2	(1,2)	.393	.796	.531	1.076
30.0	373.0	(2,3)	.111	.157	.059	.083
	1338.7	(3,4)	.007	.007	.003	.003
	4081.2	(1,2)	.151	.927	.330	2.032
	4532.8	(2,3)	.772	.706	.622	.568
40.0	391.4	(2,3)	.116	.225	.065	.127
	1544.9	(3,4)	.028	.031	.014	.015
	2689.1	(1,2)	.201	1.233	.299	1.828
	4519.5	(2,3)	.773	.735	.667	.634
50.0	422.7	(2,3)	.093	.287	.058	.180
	1929.3	(3,4)	.097	.103	.068	.072
	2331.2	(1,2)	.300	1.213	.287	1.160
	4277.0	(2,3)	.709	.756	.673	.717
60.0	475.0	(2,3)	.053	.346	.039	.254
	2147.7	(1,2)	.337	1.169	.275	.953
	2716.4	(3,4)	.293	.251	.321	.276
	3805.5	(2,3)	.595	.779	.647	.847
70.0	564.8	(2,3)	.014	.409	.014	.386
	2035.9	(1,2)	.355	1.142	.267	.860
	3143.7	(2,3)	.456	.812	.611	1.087
	3965.6	(3,4)	.649	.382	.790	.465

Table 2 (con't.)

ANGLE (Deg)	H (Oe)	TRANS.	$T_{x'}$	$T_{y'}$	$U_{x'}$	$U_{y'}$
80.0	750.0	(2,3)	.002	.504	.002	.784
	1973.4	(1,2)	.363	1.129	.262	.815
	2335.9	(2,3)	.318	.878	.640	1.769
	5006.2	(3,4)	.984	.437	1.075	.478
90.0	1953.5	(1,2)	.366	1.124	.261	.802
	5386.7	(3,4)	1.117	.452	1.162	.470

Table 3. The resonance magnetic field, the transition probability, T, and the integrated intensity, U, of Cr^{3+} ion in ruby, for microwave frequency of 14.500 GHz.

ANGLE (Deg)	H (Oe)	TRANS.	$T_{x'}$	$T_{y'}$	$U_{x'}$	$U_{y'}$
0.0	542.2	(1,4)	.000	.000	.000	.000
	1084.4	(2,4) $(-\frac{1}{2},-\frac{3}{2})$	.750	.750	.750	.750
	1742.6	(3,4)	.000	.000	.000	.000
	4685.9	(1,3)	.000	.000	.000	.000
	5227.5	(2,3) $(\frac{1}{2},-\frac{1}{2})$	1.000	1.000	1.000	1.000
	9371.6	(1,2) $(\frac{3}{2},\frac{1}{2})$	.750	.750	.750	.750
10.0	540.6	(1,4)	.016	.017	.008	.008
	1123.4	(2,4)	.724	.736	.744	.756
	1776.0	(3,4)	.003	.003	.001	.001
	4398.4	(1,3)	.332	.322	.198	.193
	5482.9	(2,3)	.893	.880	.801	.790
	9038.1	(1,2)	.703	.757	.723	.778
20.0	538.7	(1,4)	.050	.055	.024	.027
	1240.6	(2,4)	.663	.707	.721	.769
	1891.0	(3,4)	.044	.045	.017	.018
	3941.4	(1,3)	.391	.333	.240	.205
	5822.8	(2,3)	.867	.833	.753	.724
	8107.4	(1,2)	.583	.779	.650	.869
30.0	539.8	(1,4)	.077	.097	.038	.047
	1425.8	(2,4)	.590	.672	.650	.741
	2149.6	(3,4)	.182	.195	.102	.109
	3455.9	(1,3)	.342	.198	.210	.121
	6048.8	(2,3)	.870	.825	.760	.721
	6794.9	(1,2)	.452	.827	.560	1.026
40.0	548.8	(1,4)	.088	.134	.043	.065
	1646.1	(2,4)	.505	.621	.506	.623
	2681.2	(3,4)	.340	.359	.297	.313
	2914.5	(1,3)	.218	.028	.145	.018
	5457.0	(1,2)	.372	.911	.494	1.208
	6099.6	(2,3)	.866	.831	.773	.742
50.0	568.4	(1,4)	.082	.164	.041	.082
	1883.2	(2,4)	.413	.552	.368	.491
	2295.3	(1,3)	.090	.023	.072	.019
	3599.2	(3,4)	.470	.447	.525	.499
	4466.4	(1,2)	.372	1.010	.461	1.253
	5953.1	(2,3)	.844	.846	.782	.784

Table 3 (con't.)

ANGLE (Deg)	H (Oe)	TRANS.	$T_{x'}$	$T_{y'}$	$U_{x'}$	$U_{y'}$
60.0	601.6	(1,4)	.064	.189	.033	.097
	1716.8	(1,3)	.031	.113	.027	.099
	2151.2	(2,4)	.326	.470	.270	.389
	3902.3	(1,2)	.408	1.066	.438	1.145
	4819.5	(3,4)	.626	.490	.727	.569
	5624.0	(2,3)	.808	.873	.789	.852
70.0	653.5	(1,4)	.042	.209	.023	.114
	1298.4	(1,3)	.008	.167	.006	.138
	2460.2	(2,4)	.235	.359	.185	.283
	3603.5	(1,2)	.437	1.080	.420	1.038
	5173.8	(2,3)	.777	.921	.810	.961
	6039.1	(3,4)	.805	.512	.887	.565
80.0	730.9	(1,4)	.021	.233	.012	.137
	1025.8	(1,3)	.000	.179	.000	.133
	2775.0	(2,4)	.110	.174	.081	.128
	3454.7	(1,2)	.454	1.081	.410	.976
	4724.2	(2,3)	.774	1.001	.874	1.130
	6918.9	(3,4)	.953	.524	.991	.545
90.0	832.0	(1,4)	.011	.439	.007	.273
	864.8	(1,3)	.000	.000	.000	.000
	2936.7	(2,4)	.000	.000	.000	.000
	3409.4	(1,2)	.459	1.080	.407	.956
	4507.8	(2,3)	.790	1.062	.941	1.265
	7237.3	(3,4)	1.010	.527	1.027	.536

Table 4. The resonance magnetic field, the transition probability, T, and the integrated intensity, U, of Cr^{3+} ion in ruby, for microwave frequency of 18.000 GHz.

ANGLE (Deg)	H (Oe)	TRANS.	$T_{x'}$	$T_{y'}$	$U_{x'}$	$U_{y'}$
0.0	1173.0	(1,4)	.000	.000	.000	.000
	2163.3	(2,4)	.000	.000	.000	.000
	2346.1	(3,4)($-\frac{1}{2}$,$-\frac{3}{2}$)	.750	.750	.750	.750
	5316.9	(1,3)	.000	.000	.000	.000
	6489.7	(2,3)($\frac{1}{2}$,$-\frac{1}{2}$)	1.000	1.000	1.000	1.000
	10633.8	(1,2)($\frac{3}{2}$,$\frac{1}{2}$)	.750	.750	.750	.750
10.0	1165.6	(1,4)	.012	.013	.006	.006
	2202.9	(2,4)	.054	.055	.020	.020
	2420.3	(3,4)	.725	.731	.728	.734
	5110.8	(1,3)	.158	.154	.085	.083
	6657.2	(2,3)	.957	.948	.913	.904
	10329.1	(1,2)	.718	.756	.731	.770
20.0	1150.0	(1,4)	.037	.041	.018	.019
	2287.9	(2,4)	.240	.250	.108	.113
	2687.5	(3,4)	.645	.662	.641	.658
	4685.9	(1,3)	.257	.231	.146	.132
	6951.7	(2,3)	.921	.896	.844	.821
	9482.4	(1,2)	.636	.774	.681	.828
30.0	1139.5	(1,4)	.057	.069	.027	.032
	2404.3	(2,4)	.315	.342	.164	.178
	3192.2	(3,4)	.582	.601	.603	.623
	4200.8	(1,3)	.253	.183	.145	.105
	7172.9	(2,3)	.910	.876	.825	.794
	8286.6	(1,2)	.542	.809	.617	.921
40.0	1143.0	(1,4)	.065	.093	.030	.042
	2563.7	(2,4)	.319	.366	.181	.208
	3685.9	(1,3)	.188	.080	.109	.046
	3973.4	(3,4)	.572	.569	.629	.627
	7027.3	(1,2)	.476	.864	.564	1.024
	7240.7	(2,3)	.902	.873	.825	.799
50.0	1166.0	(1,4)	.061	.111	.028	.050
	2773.8	(2,4)	.291	.355	.175	.214
	3146.1	(1,3)	.101	.007	.061	.004
	5032.2	(3,4)	.618	.557	.701	.632
	5981.4	(1,2)	.456	.931	.531	1.083
	7127.9	(2,3)	.888	.884	.831	.827

Table 4 (con't.)

ANGLE (Deg.)	H (Oe)	TRANS.	$T_{x'}$	$T_{y'}$	$U_{x'}$	$U_{y'}$
60.0	1213.7	(1,4)	.050	.125	.023	.057
	2623.0	(1,3)	.038	.008	.024	.005
	3035.9	(2,4)	.244	.315	.153	.197
	5271.5	(1,2)	.469	.985	.510	1.069
	6254.9	(3,4)	.713	.556	.795	.619
	6850.6	(2,3)	.869	.908	.843	.881
70.0	1291.2	(1,4)	.034	.136	.016	.064
	2181.2	(1,3)	.009	.037	.006	.023
	3335.2	(2,4)	.172	.232	.109	.147
	4851.6	(1,2)	.490	1.013	.493	1.021
	6469.7	(2,3)	.857	.949	.871	.965
	7405.3	(3,4)	.831	.558	.887	.595
80.0	1404.3	(1,4)	.019	.154	.009	.076
	1849.6	(1,3)	.000	.050	.000	.030
	3613.3	(2,4)	.070	.096	.043	.059
	4634.0	(1,2)	.504	1.024	.483	.982
	6106.4	(2,3)	.863	1.006	.923	1.077
	8221.7	(3,4)	.928	.560	.952	.574
90.0	1514.5	(1,4)	.013	.230	.006	.111
	1667.6	(1,3)	.000	.000	.000	.000
	3739.1	(2,4)	.000	.000	.000	.000
	4567.2	(1,2)	.509	1.027	.479	.968
	5944.3	(2,3)	.873	1.040	.961	1.145
	8516.0	(3,4)	.966	.561	.976	.567

Table 5. The resonance magnetic field, the transition probability, T, and the integrated intensity, U, of Cr^{3+} ion in ruby, for microwave frequency of 24.000 GHz.

ANGLE (Deg)	H (Oe)	TRANS.	$T_{x'}$	$T_{y'}$	$U_{x'}$	$U_{y'}$
0.0	2254.7	(1,4)	.000	.000	.000	.000
	2884.4	(2,4)	.000	.000	.000	.000
	4509.4	(3,4)($-\frac{1}{2}$,$-\frac{3}{2}$)	.750	.750	.750	.750
	6398.4	(1,3)	.000	.000	.000	.000
	8653.3	(2,3)($\frac{1}{2}$,$-\frac{1}{2}$)	1.000	1.000	1.000	1.000
	12796.9	(1,2)($\frac{3}{2}$,$\frac{1}{2}$)	.750	.750	.750	.750
10.0	2220.3	(1,4)	.008	.008	.004	.004
	2963.3	(2,4)	.004	.004	.001	.001
	4609.4	(3,4)	.742	.743	.749	.750
	6245.6	(1,3)	.059	.058	.030	.030
	8759.3	(2,3)	.985	.980	.967	.963
	12521.5	(1,2)	.731	.754	.738	.762
20.0	2155.9	(1,4)	.023	.024	.010	.011
	3153.7	(2,4)	.033	.035	.013	.014
	4928.1	(3,4)	.719	.720	.744	.745
	5871.8	(1,3)	.134	.125	.071	.066
	8983.4	(2,3)	.961	.946	.919	.905
	11755.9	(1,2)	.681	.768	.706	.797
30.0	2104.7	(1,4)	.033	.039	.014	.017
	3396.1	(2,4)	.089	.096	.040	.043
	5397.0	(1,3)	.155	.128	.084	.069
	5502.0	(3,4)	.694	.686	.738	.729
	9177.7	(2,3)	.947	.925	.893	.872
	10664.6	(1,2)	.620	.793	.665	.850
40.0	2083.2	(1,4)	.037	.050	.015	.021
	3667.6	(2,4)	.138	.155	.067	.075
	4883.2	(1,3)	.132	.087	.071	.047
	6350.6	(3,4)	.687	.652	.744	.706
	9252.0	(2,3)	.938	.918	.884	.865
	9475.6	(1,2)	.572	.829	.626	.907
50.0	2097.3	(1,4)	.035	.058	.014	.024
	3965.2	(2,4)	.158	.184	.083	.097
	4359.0	(1,3)	.086	.035	.046	.019
	7428.7	(3,4)	.713	.627	.773	.680
	8407.2	(1,2)	.549	.871	.598	.949
	9172.9	(2,3)	.930	.924	.887	.881

Table 5 (con't.)

ANGLE (Deg)	H (Oe)	TRANS.	$T_{x'}$	$T_{y'}$	$U_{x'}$	$U_{y'}$
60.0	2149.6	(1,4)	.028	.063	.012	.026
	3853.9	(1,3)	.043	.006	.023	.003
	4285.9	(2,4)	.145	.175	.079	.096
	7590.8	(1,2)	.547	.910	.579	.963
	8606.0	(3,4)	.769	.612	.820	.652
	8953.1	(2,3)	.923	.942	.900	.919
70.0	2241.4	(1,4)	.019	.066	.008	.027
	3407.8	(1,3)	.015	.000	.008	.000
	4606.6	(2,4)	.100	.124	.056	.069
	7049.8	(1,2)	.555	.938	.565	.956
	8651.4	(2,3)	.921	.972	.925	.976
	9676.8	(3,4)	.838	.604	.870	.627
80.0	2365.0	(I,4)	.011	.072	.004	.030
	3060.5	(1,3)	.002	.003	.001	.001
	4867.2	(2,4)	.036	.045	.020	.025
	6749.0	(1,2)	.563	.953	.557	.943
	8376.5	(2,3)	.927	1.005	.959	1.040
	10425.8	(3,4)	.895	.601	.907	.609
90.0	2448.8	(1,4)	.007	.082	.003	.033
	2900.8	(1,3)	.000	.000	.000	.000
	4972.3	(2,4)	.000	.000	.000	.000
	6653.3	(1,2)	.566	.957	.554	.937
	8261.2	(2,3)	.932	1.022	.978	1.073
	10695.3	(3,4)	.917	.600	.921	.603

Table 6. The resonance magnetic field, the transition probability, T, and the integrated intensity, U, of Cr^{3+} ion in ruby, for microwave frequency of 35.000 GHz.

ANGLE (Deg)	H (Oe)	TRANS.	$T_{x'}$	$T_{y'}$	$U_{x'}$	$U_{y'}$
0.0	4206.2	(1,4)	.000	.000	.000	.000
	4237.5	(2,4)	.000	.000	.000	.000
	8381.3	(1,3)	.000	.000	.000	.000
	8475.6	(3,4)($-\frac{1}{2}$,$-\frac{3}{2}$)	.750	.750	.750	.750
	12619.1	(2,3)($\frac{1}{2}$,$-\frac{1}{2}$)	1.000	1.000	1.000	1.000
	16762.7	(1,2)($\frac{3}{2}$,$\frac{1}{2}$)	.750	.750	.750	.750
10.0	3991.8	(1,4)	.002	.002	.001	.001
	4507.4	(2,4)	.004	.004	.002	.002
	8259.8	(1,3)	.019	.019	.010	.010
	8603.0	(3,4)	.747	.746	.751	.749
	12684.6	(2,3)	.995	.993	.989	.986
	16515.4	(1,2)	.740	.753	.743	.757
20.0	3820.3	(1,4)	.007	.008	.003	.003
	4839.1	(2,4)	.018	.019	.008	.009
	7933.6	(1,3)	.054	.052	.028	.026
	8990.7	(3,4)	.741	.733	.753	.745
	12835.9	(2,3)	.984	.977	.966	.959
	15822.8	(1,2)	.713	.763	.725	.776
30.0	3706.6	(1,4)	.011	.013	.004	.005
	5206.1	(2,4)	.041	.044	.019	.020
	7479.0	(1,3)	.074	.067	.038	.034
	9644.5	(3,4)	.736	.714	.759	.736
	12982.9	(2,3)	.975	.963	.947	.936
	14819.3	(1,2)	.679	.779	.700	.804
40.0	3649.0	(1,4)	.013	.017	.005	.006
	5595.2	(2,4)	.064	.070	.031	.034
	6962.2	(1,3)	.072	.058	.037	.030
	10545.4	(3,4)	.741	.692	.770	.720
	13049.8	(2,3)	.968	.957	.938	.927
	13689.5	(1,2)	.649	.802	.675	.835
50.0	3644.7	(1,4)	.013	.020	.005	.007
	5994.6	(2,4)	.075	.085	.038	.043
	6429.7	(1,3)	.055	.037	.028	.019
	11624.5	(3,4)	.759	.673	.790	.700
	12613.3	(1,2)	.629	.827	.655	.861
	12999.0	(2,3)	.964	.960	.938	.934

Table 6 (con't.)

ANGLE (Deg)	H (Oe)	TRANS.	$T_{x'}$	$T_{y'}$	$U_{x'}$	$U_{y'}$
60.0	3690.4	(1,4)	.010	.021	.004	.008
	5919.4	(1,3)	.033	.017	.017	.009
	6386.0	(2,4)	.069	.080	.036	.041
	11722.2	(1,2)	.621	.852	.639	.877
	12750.0	(3,4)	.791	.658	.815	.678
	12840.8	(2,3)	.962	.970	.947	.956
70.0	3777.3	(1,4)	.006	.020	.002	.008
	5472.2	(1,3)	.014	.005	.007	.003
	6736.1	(2,4)	.045	.053	.024	.028
	11080.1	(1,2)	.621	.871	.629	.883
	12624.0	(2,3)	.963	.987	.964	.987
	13744.6	(3,4)	.827	.648	.842	.660
80.0	3879.1	(1,4)	.003	.019	.001	.007
	5142.6	(1,3)	.003	.001	.002	.000
	6989.7	(2,4)	.015	.018	.008	.009
	10700.2	(1,2)	.623	.884	.622	.883
	12433.6	(2,3)	.967	1.003	.981	1.018
	14429.7	(3,4)	.856	.643	.862	.647
90.0	3930.9	(1,4)	.002	.019	.001	.007
	5012.7	(1,3)	.000	.000	.000	.000
	7084.2	(2,4)	.000	.000	.000	.000
	10575.2	(1,2)	.624	.888	.620	.883
	12356.9	(2,3)	.969	1.010	.990	1.032
	14673.8	(3,4)	.867	.641	.869	.642

Table 7. The resonance magnetic field, the transition probability, T, and the integrated intensity, U, of Cr^{3+} ion in ruby, for microwave frequency of 50.000 GHz.

ANGLE (Deg.)	H (Oe)	TRANS.	$T_{x'}$	$T_{y'}$	$U_{x'}$	$U_{y'}$
0.0	6009.0	(1,4)	.000	.000	.000	.000
	6941.9	(2,4)	.000	.000	.000	.000
	11085.4	(1,3)	.000	.000	.000	.000
	13883.8	(3,4)($-\frac{1}{2}$,$-\frac{3}{2}$)	.750	.750	.750	.750
	18027.3	(2,3)($\frac{1}{2}$,$-\frac{1}{2}$)	1.000	1.000	1.000	1.000
	22170.9	(1,2)($\frac{3}{2}$,$\frac{1}{2}$)	.750	.750	.750	.750
10.0	5938.0	(1,4)	.000	.000	.000	.000
	7076.4	(2,4)	.003	.003	.002	.002
	10977.5	(1,3)	.007	.007	.004	.004
	14029.3	(3,4)	.749	.747	.751	.749
	18070.3	(2,3)	.998	.997	.995	.994
	21941.4	(1,2)	.744	.752	.746	.754
20.0	5803.7	(1,4)	.001	.001	.000	.001
	7396.5	(2,4)	.011	.012	.006	.006
	10676.8	(1,3)	.023	.022	.012	.011
	14462.4	(3,4)	.749	.739	.755	.745
	18175.8	(2,3)	.993	.989	.984	.981
	21295.4	(1,2)	.729	.759	.735	.766
30.0	5689.2	(1,4)	.003	.003	.001	.001
	7806.2	(2,4)	.023	.024	.011	.012
	10237.8	(1,3)	.035	.033	.018	.017
	15168.0	(3,4)	.750	.726	.761	.737
	18282.7	(2,3)	.988	.982	.974	.968
	20346.7	(1,2)	.708	.771	.719	.782
40.0	5622.1	(1,4)	.004	.005	.001	.002
	8257.3	(2,4)	.033	.036	.016	.018
	9721.2	(1,3)	.038	.033	.019	.017
	16103.5	(3,4)	.757	.712	.772	.726
	18335.0	(2,3)	.984	.978	.968	.962
	19252.0	(1,2)	.689	.786	.703	.801
50.0	5608.2	(1,4)	.004	.006	.001	.002
	8717.3	(2,4)	.038	.042	.019	.021
	9180.2	(1,3)	.031	.025	.016	.013
	17182.6	(3,4)	.771	.698	.786	.711
	18173.8	(1,2)	.674	.802	.688	.818
	18301.8	(2,3)	.981	.979	.967	.965

Table 7 (con't.)

ANGLE (Deg)	H (Oe)	TRANS.	$T_{x'}$	$T_{y'}$	$U_{x'}$	$U_{y'}$
60.0	5643.8	(1,4)	.003	.006	.001	.002
	8663.6	(1,3)	.021	.015	.010	.008
	9153.3	(2,4)	.034	.038	.017	.019
	17242.2	(1,2)	.666	.819	.676	.830
	18187.5	(2,3)	.981	.985	.973	.977
	18274.4	(3,4)	.790	.686	.802	.697
70.0	5714.4	(1,4)	.002	.006	.001	.002
	8220.7	(1,3)	.010	.006	.005	.003
	9523.4	(2,4)	.021	.024	.011	.012
	16541.0	(1,2)	.663	.832	.667	.838
	18031.8	(2,3)	.982	.994	.982	.993
	19218.7	(3,4)	.811	.678	.818	.683
80.0	5789.3	(1,4)	.001	.005	.000	.002
	7910.6	(1,3)	.003	.001	.001	.001
	9777.1	(2,4)	.007	.008	.003	.004
	16110.8	(1,2)	.662	.841	.662	.841
	17897.9	(2,3)	.984	1.002	.991	1.009
	19861.3	(3,4)	.827	.673	.830	.675
90.0	5823.2	(1,4)	.000	.005	.000	.002
	7796.4	(1,3)	.000	.000	.000	.000
	9868.2	(2,4)	.000	.000	.000	.000
	15966.8	(1,2)	.662	.844	.661	.842
	17844.7	(2,3)	.985	1.005	.995	1.015
	20088.9	(3,4)	.833	.671	.834	.671

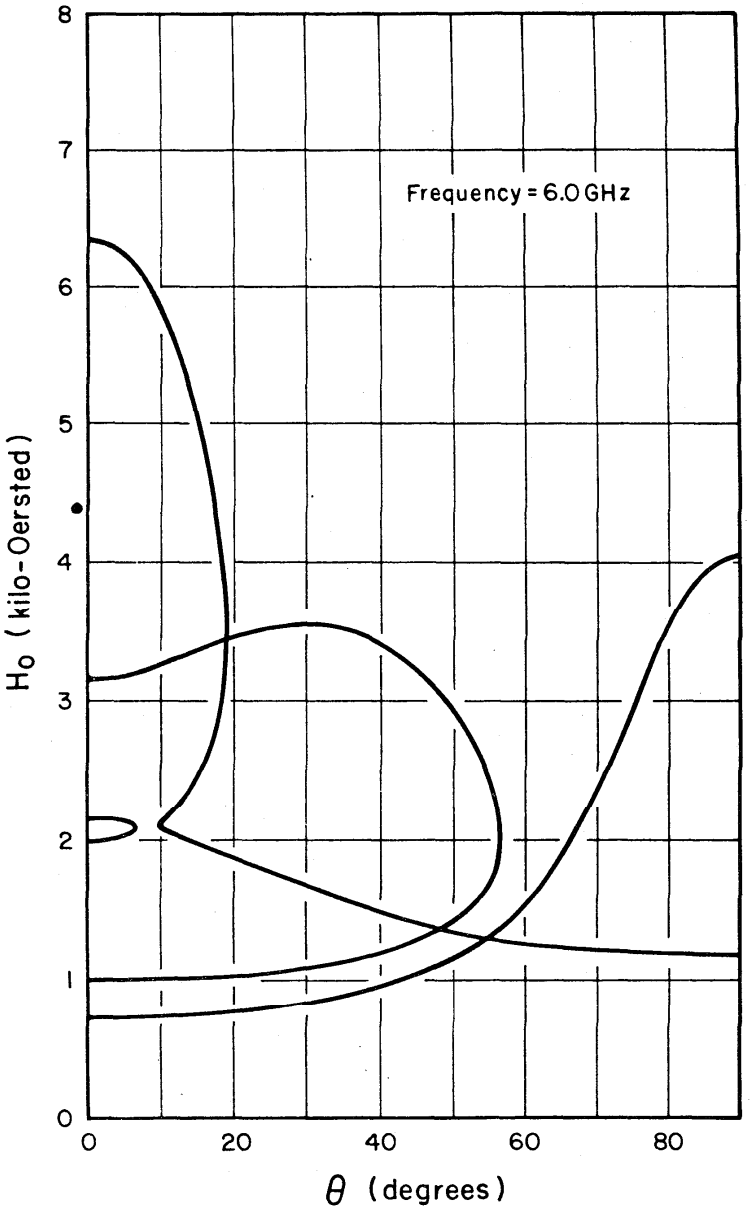

Fig. 1. Paramagnetic resonance spectrum of Cr^{3+} in ruby for a transition frequency of 6.0 GHz. Plots give the values of the resonance fields, H_o, as a function of θ, the angle between the c-axis of the ruby SRM and the direction of the field, H_o.

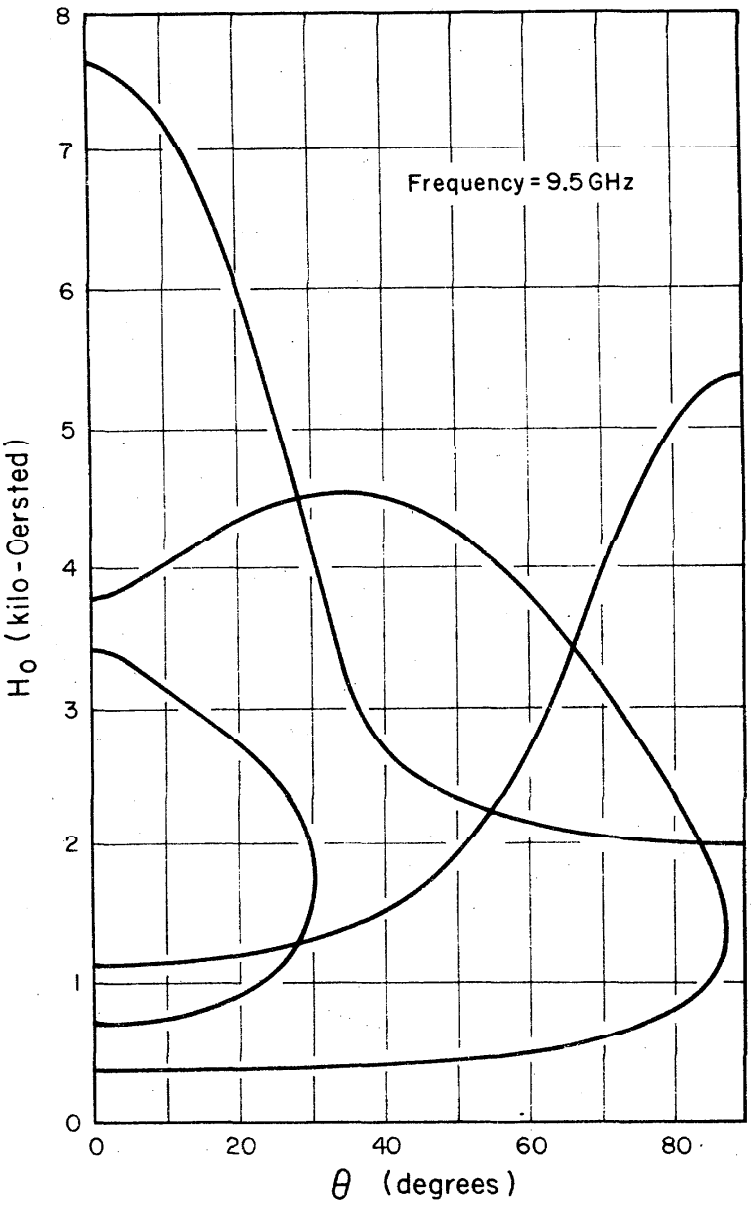

Fig. 2. Paramagnetic resonance spectrum of Cr^{3+} in ruby for a transition frequency of 9.5 GHz. Plots give the values of the resonance fields, H_o, as a function of θ, the angle between the c-axis of the ruby SRM and the direction of the field, H_o.

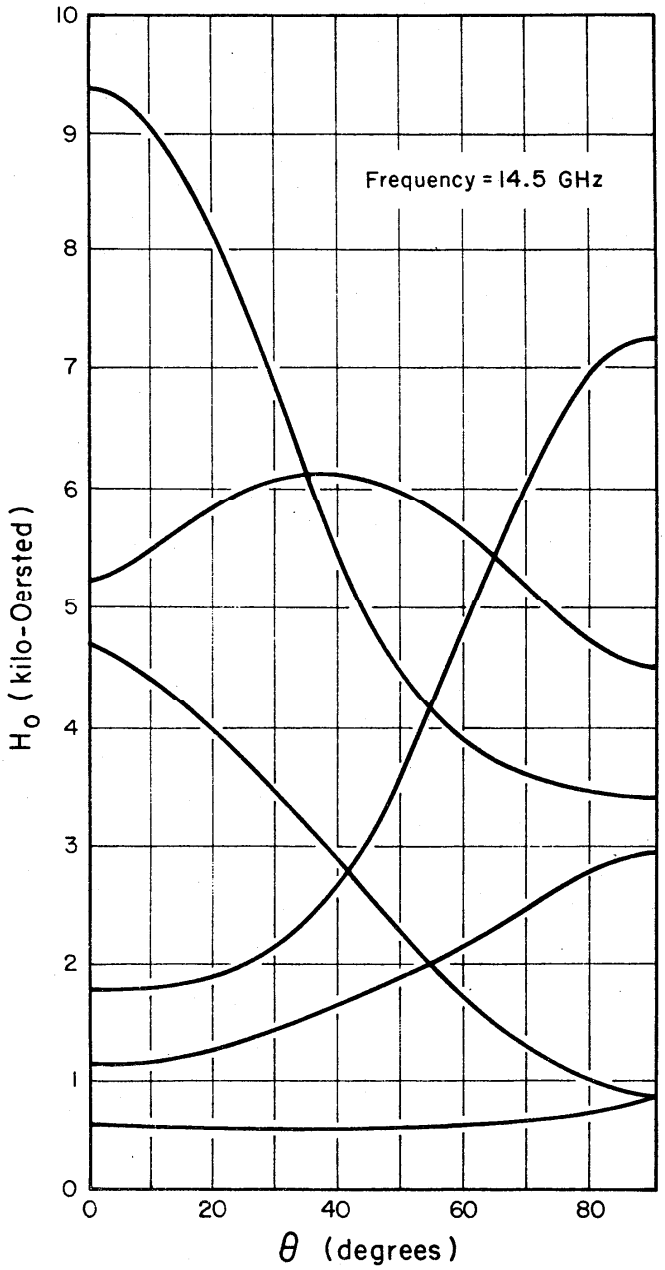

Fig. 3. Paramagnetic resonance spectrum of Cr^{3+} in ruby for a transition frequency of 14.5 GHz. Plots give the values of the resonance fields, H_o, as a function of θ, the angle between the c-axis of the ruby SRM and the direction of the field, H_o.

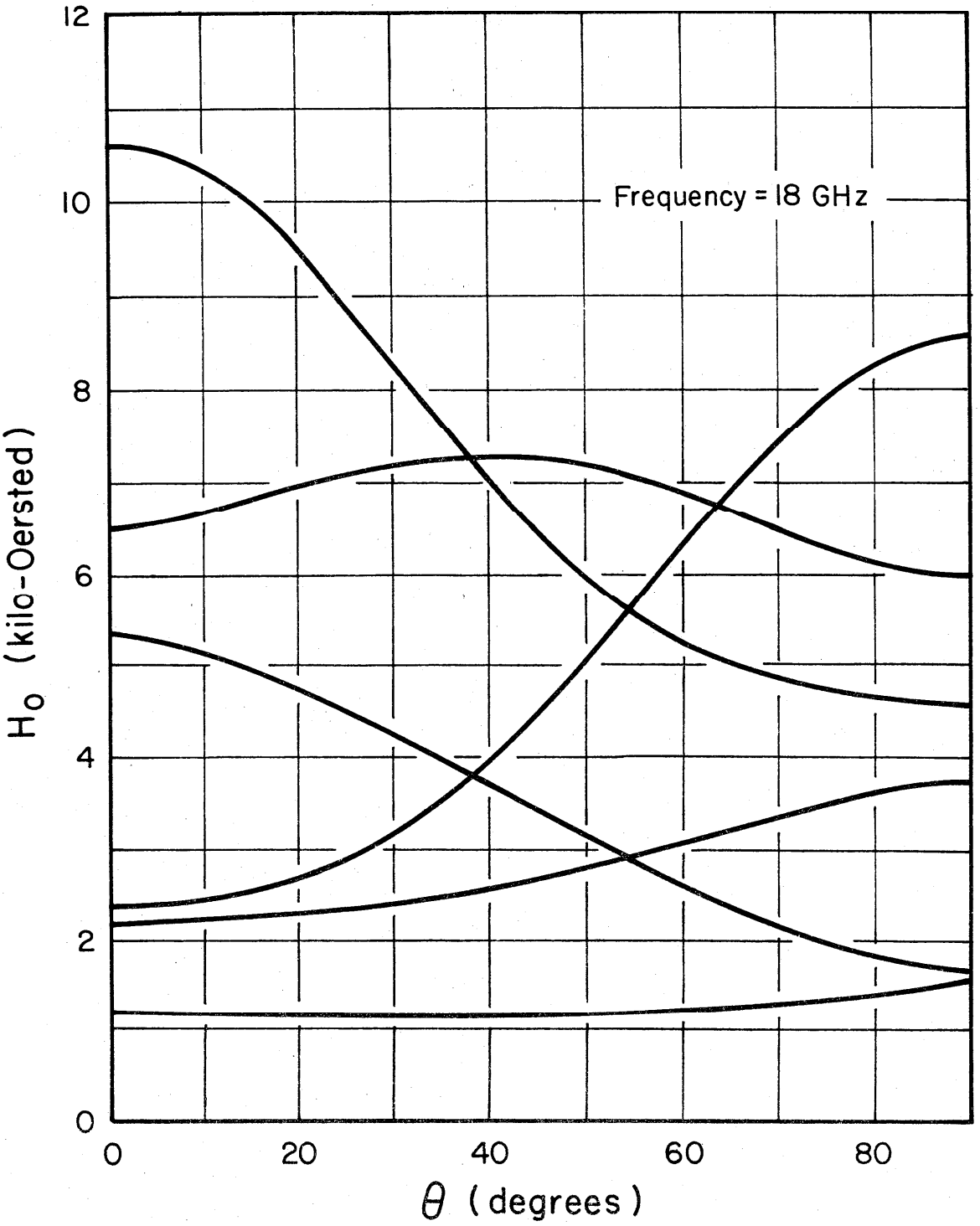

Fig. 4. Paramagnetic resonance spectrum of Cr^{3+} in ruby for a transition frequency of 18.0 GHz. Plots give the values of the resonance fields, H_o, as a function of θ, the angle between the c-axis of the ruby SRM and the direction of the field, H_o.

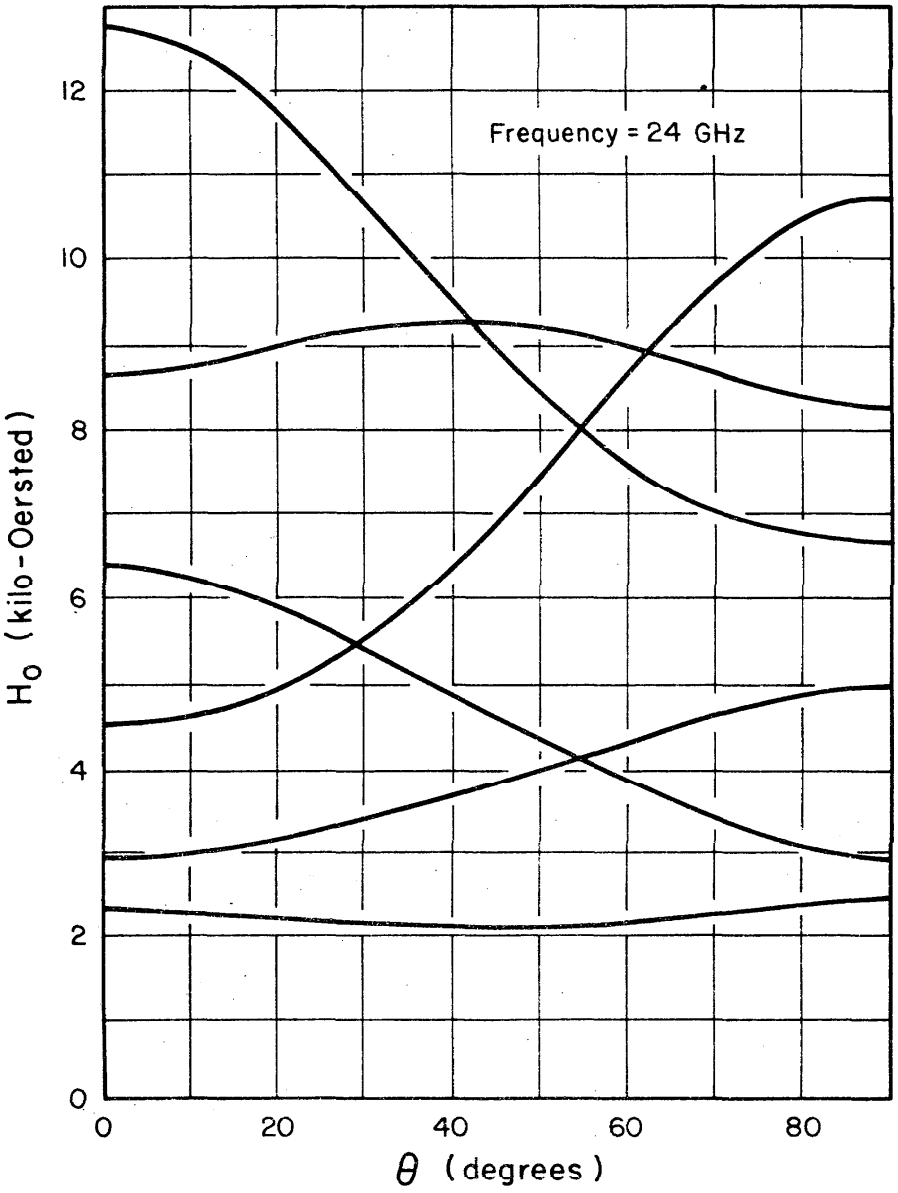

Fig. 5. Paramagnetic resonance spectrum of Cr^{3+} in ruby for a transition frequency of 24.0 GHz. Plots give the values of the resonance fields, H_o, as a function of θ, the angle between the c-axis of the ruby SRM and the direction of the field, H_o.

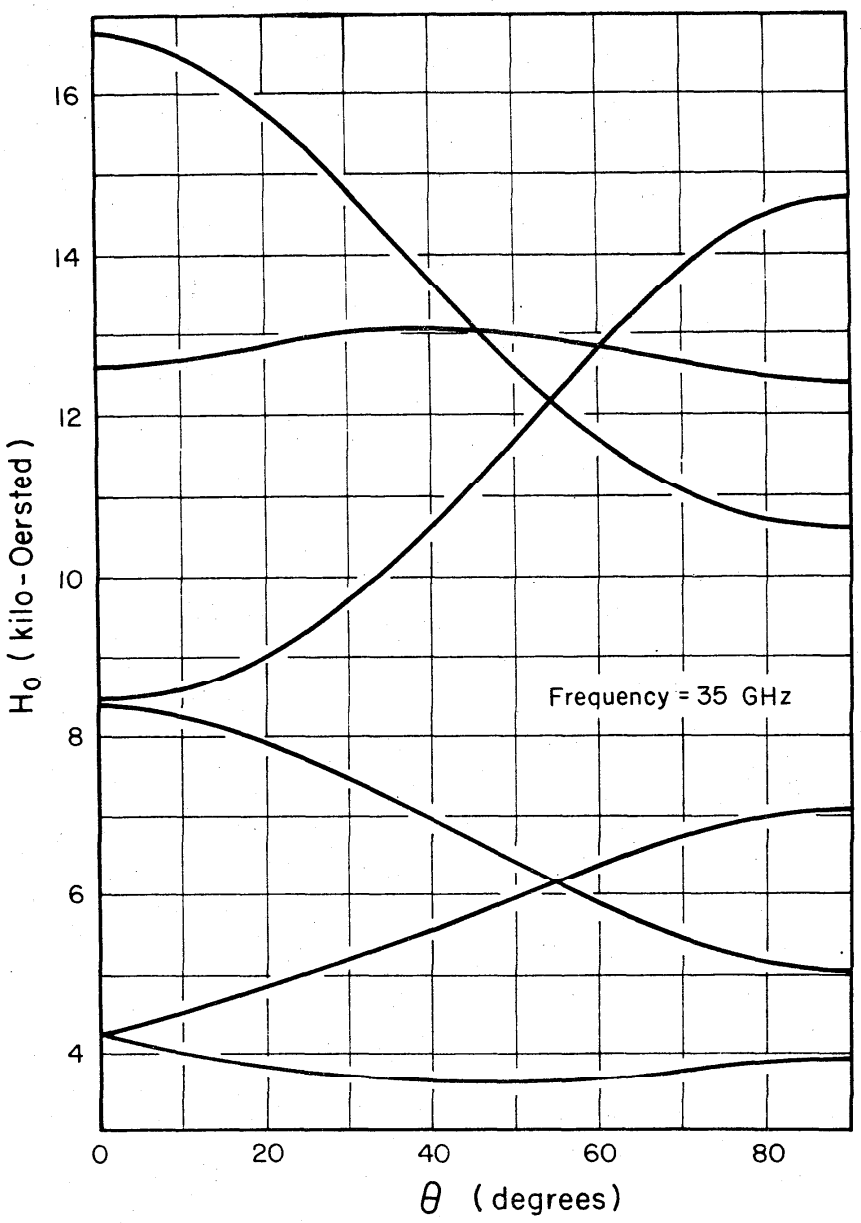

Fig. 6. Paramagnetic resonance spectrum of Cr^{3+} in ruby for a transition frequency of 35.0 GHz. Plots give the values of the resonance fields, H_o, as a function of θ, the angle between the c-axis of the ruby SRM and the direction of the field, H_o.

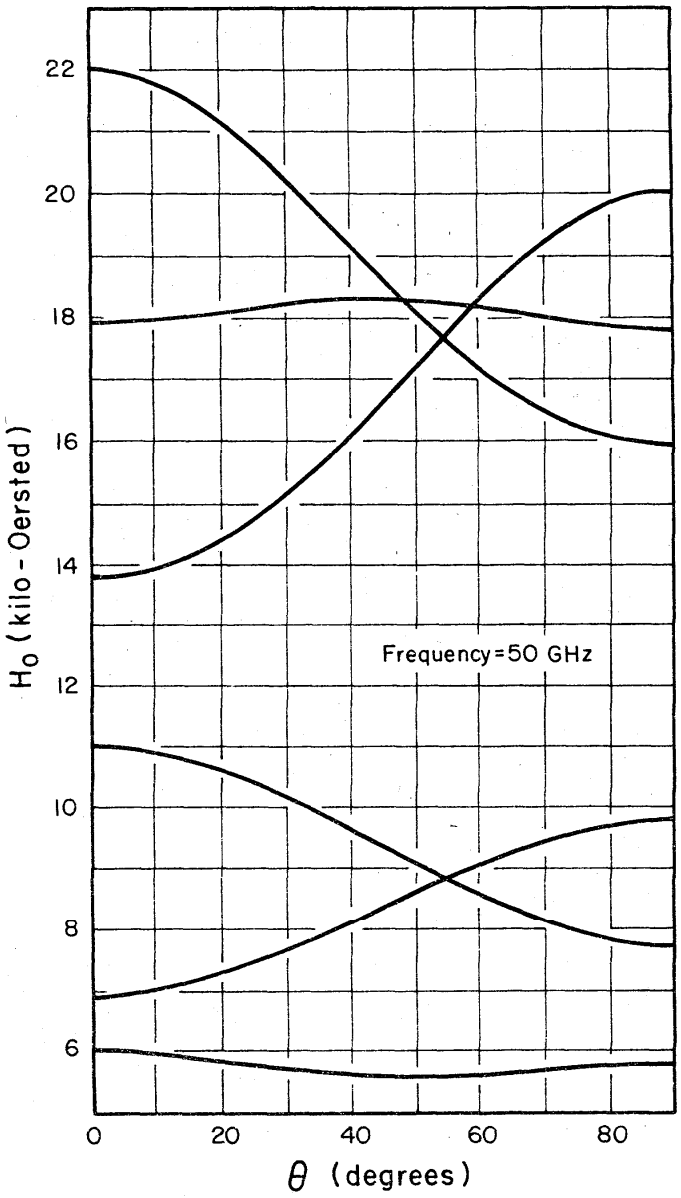

Fig. 7. Paramagnetic resonance spectrum of Cr^{3+} in ruby for a transition frequency of 50.0 GHz. Plots give the values of the resonance fields, H_o, as a function of θ, the angle between the c-axis of the ruby SRM and the direction of the field, H_o.

For a visual display of the resonance fields versus angle θ, at each microwave frequency, we have prepared the graphs of Fig. 1 through Fig. 7. These plots give the resonance fields only. The intensities and other information can be obtained from the tables.

3. Description of the Ruby EPR SRM

3.1 Physical Description

Each set of EPR SRM consists of two pieces of ruby single crystal. One piece is a square wafer of dimensions approximately 1.5 x 1.5 x 0.5 mm, with the c-axis perpendicular to the square surface. The second piece is a bar of dimensions approximately 0.5 x 0.5 x 4.0 mm, with the c-axis parallel to the long edge. The orientation of the c-axis, with respect to the specified direction, has a maximum error of 0.5°. The dimensions are nominal. The total number of Cr^{3+} ions in each piece is given in the accompanying certificate.

The SRM specimens were cut from a single crystal boule, annealed at 1800 °C, and etched in hot concentrated phosphoric acid at 500 °C. The surface appears wavy and glazed. The color is a pale pink. The annealing and etching treatments were necessary for obtaining consistent EPR spectra. Details are discussed in another publication [7].

3.2 Packaging

Each ruby SRM specimen is contained in a plastic vial. The two vials are contained in a plastic bottle. We recommend storing the specimens in the packing containers when they are not in use. This precautionary advice is offered because the specimens, being small and transparent, are easily lost.

3.3 Handling

The ruby SRM should be handled with fine tweezers, preferably non-magnetic (e.g. brass, German silver, or plastic tweezers). Steel tweezers may leave undesirable ferrous contamination on the surface of the ruby.

Instructions for initial inspection are as follows:

1. Remove the two vials from the plastic bottle. The ruby samples are visible through the walls of the plastic vials.

2. Prepare a shallow glass dish, such as a culture dish or evaporation dish, and place a white or dark background under the dish to provide contrast for ease of viewing. Provide adequate lighting.

3. Select one of the vials for opening and place it in the dish. Open the cap smoothly so that the crystal will not fly out.

4. The SRM specimen can be taken from the vial with tweezers, or it can be dumped out into the dish by pressing the mouth of the vial to the dish and lightly tapping the bottom. Care should be exercised to prevent the crystal from being lost.

5. Inspect and return the SRM to the containers.

3.4 Cleaning

The surface of the ruby specimen can be cleaned by wiping with paper or cotton soaked with an organic solvent, such as alcohol or acetone. If the surface needs to be scrubbed, the sample should be soaked in the appropriate solvent for easier cleaning.

If there is confirmed metallic contamination on the surface, dilute hydrochloric acid may be used to remove it. The sample must be throughly rinsed afterward. However, it is not necessary to wash the samples in acid routinely.

4. Positioning the SRM in the Cavity

In this chapter, we shall suggest methods for the mounting of the ruby SRM in the sample cavity. In usual practice the sample cavity is arranged so that the microwave magnetic field is vertical. The DC magnetic field produced by the magnet is usually horizontal. From this assumed configuration, we shall develop a method to determine the orientation of the laboratory coordinate system x'y'z', and hence to determine the integrated intensity factor, $U_{x'}$ or $U_{y'}$, to be used in the measurement. It is important that the user examine his spectrometer and determine whether there is any difference between the spectrometer configuration and that which is described here. Necessary modifications to suit the individual case in question should be made.

4.1 The Microwave Cavity

We shall discuss three types of microwave cavities commonly used in EPR experiments.

4.1.1 Rectangular cavity, TE_{102} mode. The TE_{102} rectangular cavity is essentially a piece of rectangular waveguide stopped at both ends, as shown in Fig. 8 and Fig. 9. The coupling iris is the hole shown at one end; this end is connected to the waveguide from the external microwave system. A variable coupling adjustment is usually placed outside the cavity in the connecting waveguide. The dashed lines of Figs. 8 and 9 represent the loops of the RF magnetic lines of force. The magnetic field decreases toward the center of the loops. At the center, the RF magnetic field is zero, and the RF electric field is a maximum.

An experimental sample can be placed at the positions shown. These positions are the locations of the maximum RF magnetic field. However, the loops tend to round off at the corners. Hence, unless the sample is small, there will be a variation of magnetic field over the volume of the sample.

The TE_{102} cavity can be used vertically as in Fig. 8, or horizontally as in Fig. 9. In the vertical configuration the sample can be attached to the cavity wall. In the horizontal configuration a sample holder is needed. The sample holder can be fashioned from a quartz or other dielectric rod, a tube, or a square cell.

4.1.2 Cylindrical cavity, TE_{011} mode. The TE_{011} cylindrical cavity is a piece of cylindrical pipe stopped by two end plates as shown in Fig. 10. The iris can be on the end plate half-way between the center and the side wall, or on the side wall at half the height of the cylinder. The quality factor (Q) is a maximum when the diameter is equal to the height. The sample can be placed at the position shown and supported by a sample holder. This type of cavity usually has a high Q and a large volume. A large sample access hole can be cut at the center of an end plate without disturbing the cavity mode.

4.1.3 Cylindrical cavity, TM_{110} mode. The cylindrical cavity in the TM_{110} mode is shown in Fig. 11. It has a microwave magnetic field pattern that is not cylindrically symmetric, as shown. This mode can only be excited through an iris on the side wall. The frequency of the cavity is determined by the diameter only. The length of the cavity is arbitrary, and it can be very long. This type of cavity can accommodate a very large sample.

4.2 Adhesives

The SRM can best be attached to a surface or a sample holder with adhesives. Either varnish or household cement may be used. The adhesive should be of a type that is removable by washing with an organic solvent. Cement that can form a permanent bond must not be used. The low temperature glue commonly used in EPR research are satisfactory. We recommend that a trial application of the adhesive on a similar surface be performed before it is used on the SRM.

Most adhesives have or tend to form broken chemical bonds or free radicals that will produce EPR signals. It is advisable to dilute the adhesives with the appropriate solvent to reduce the amount of cement used as well as to speed the drying. Of course, this procedure will only lessen the possible interference from the adhesive. A blank run with adhesive only will determine if there is any extraneous signal.

4.3 Sample Mounting and Associated RF Polarization

It is of utmost importance in the use of the ruby SRM that the user know the orientations of the c-axis, the static magnetic field, H_o, and the direction of polarization of the RF magnetic field, H_1. In the

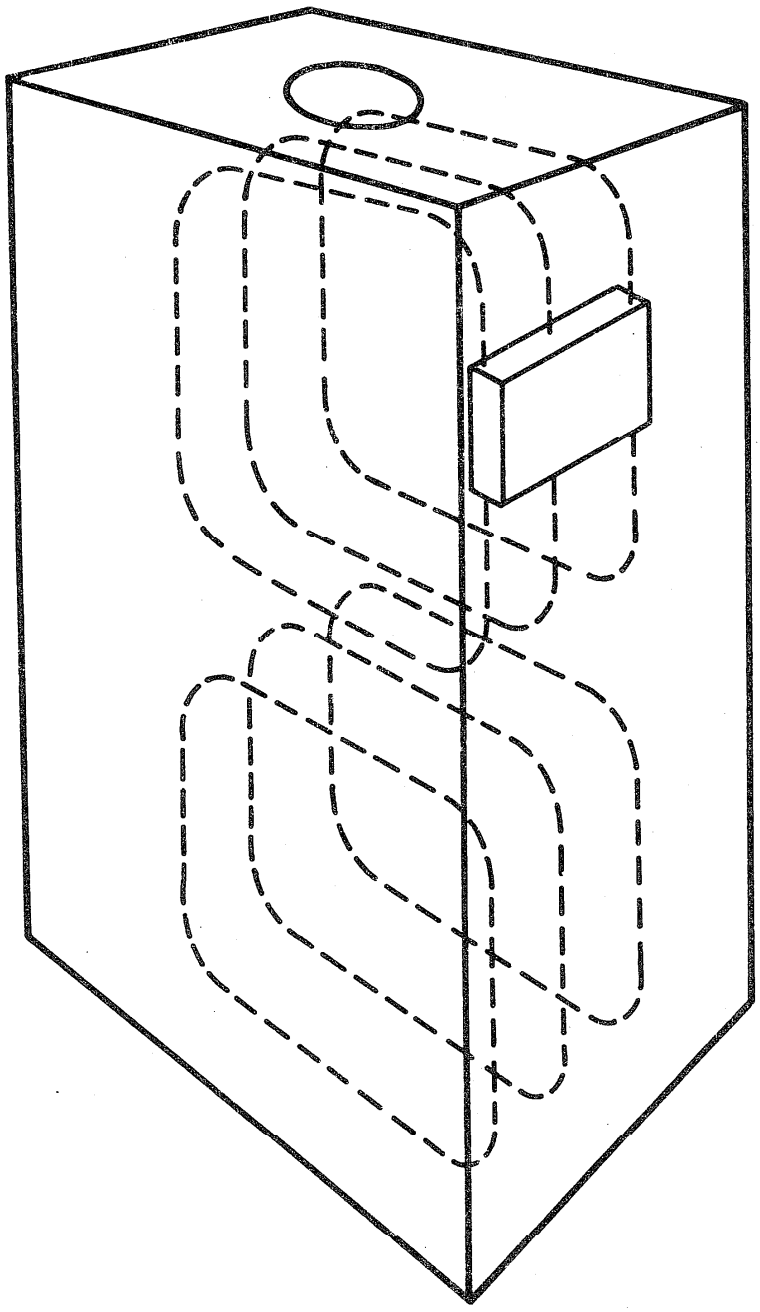

Fig. 8. Rectangular cavity, TE_{102} mode. Dashed lines represent the RF magnetic field. The square plate represents the sample which is attached to the wall. The circle on the top face represents the coupling iris.

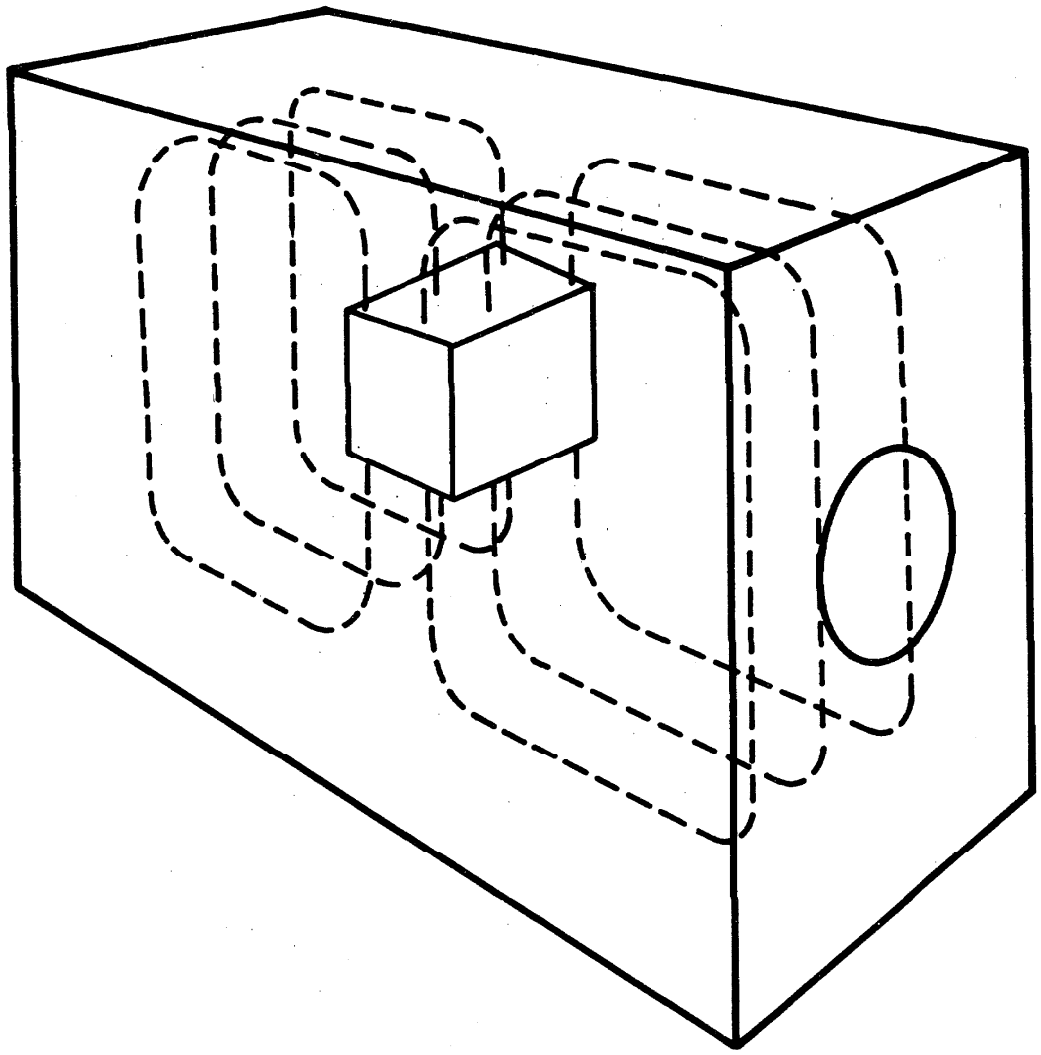

Fig. 9. Rectangular cavity, TE_{102} mode. Dashed lines represent the RF magnetic field. The rectangular block represents the sample, which must be supported. The circle on the end represents the coupling iris.

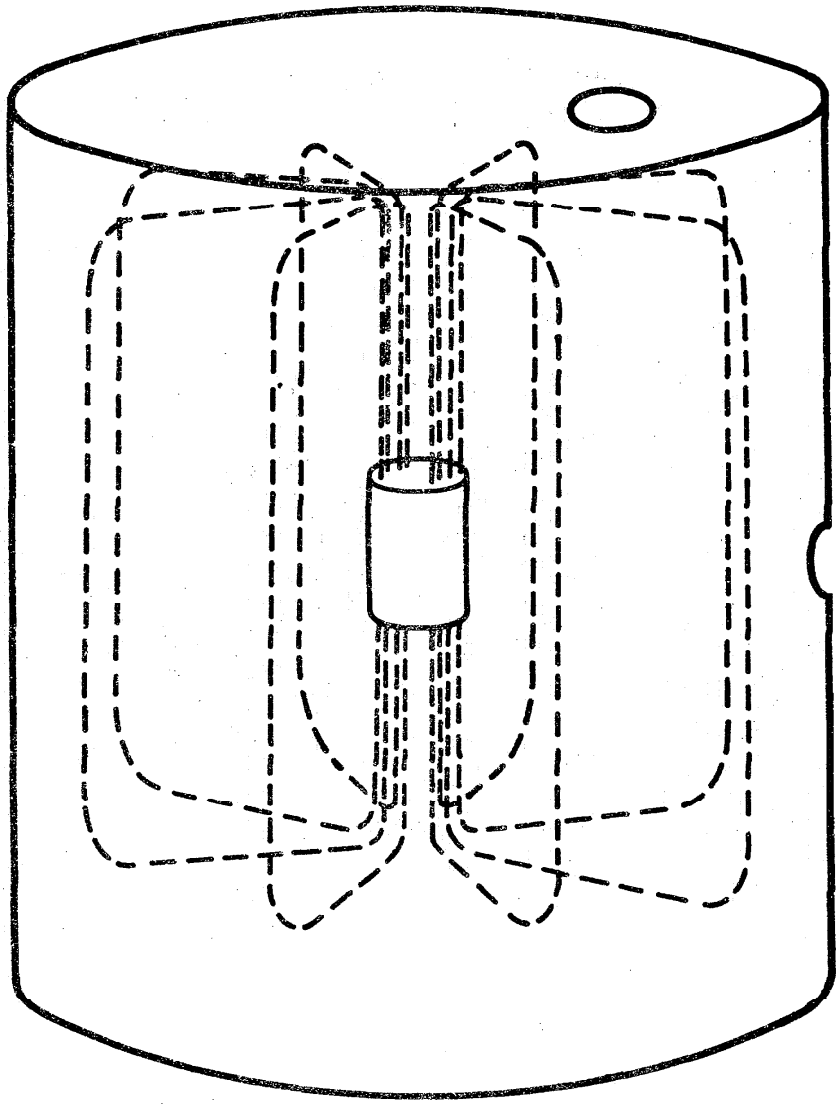

Fig. 10. Cylindrical cavity, TE_{011} mode. Dashed lines represent the RF magnetic field. The small cylinder at the center represents the sample, which must be supported. The circles on the top and side represent possible locations of the coupling iris.

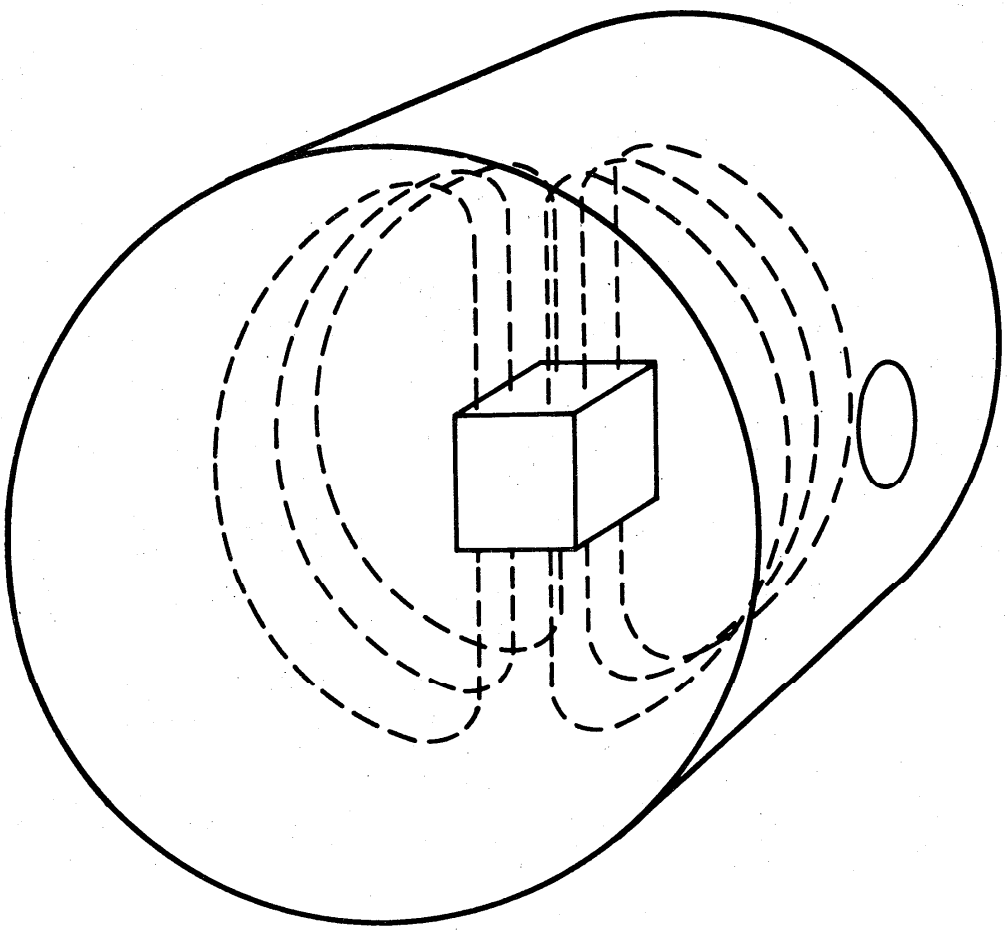

Fig. 11. Cylindrical cavity, TM_{110} mode. Dashed lines represent the RF magnetic field. The rectangular block at the center represents the sample, which must be supported. The circle on the side represents the coupling iris.

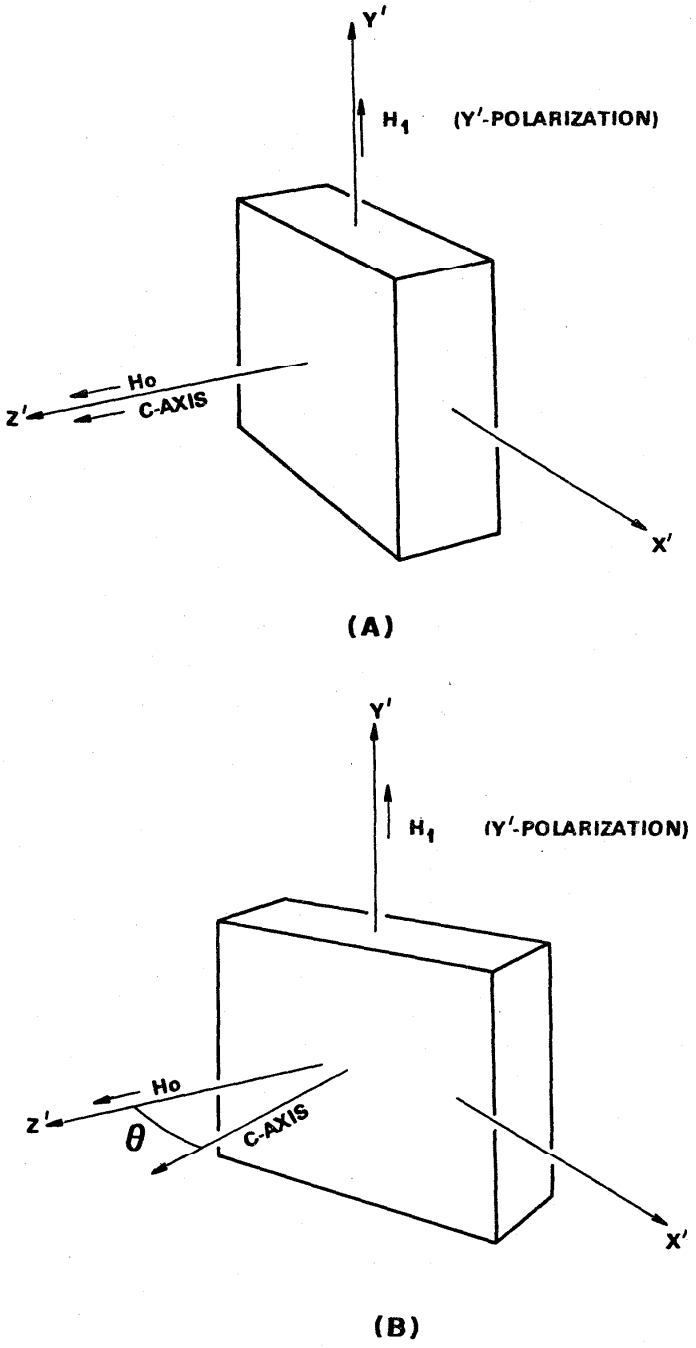

Fig. 12. Schematic drawings demonstrating the relative orientation of the wafer SRM and the laboratory coordinate system x'y'z'. In (A) the c-axis is parallel to the direction of the DC field, H_o, and the RF field, H_1, has Y'-polarization. In (B) the c-axis makes arbitrary angle θ with the direction of H_o and the RF field is shown with Y'-polarization.

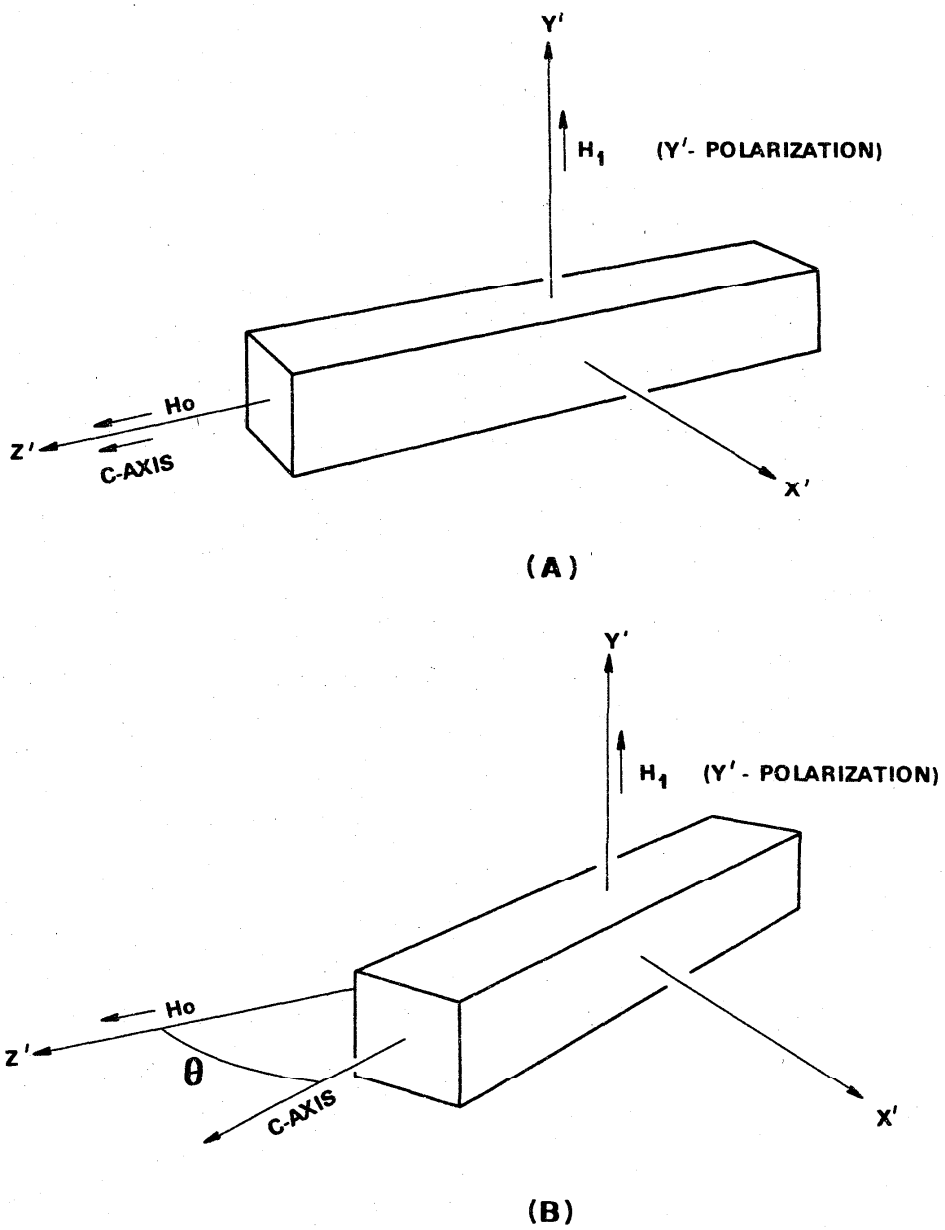

Fig. 13. Schematic drawings demonstrating the relative orientation of the bar SRM and the laboratory coordinate system x'y'z'. In (A) the c-axis is parallel to the direction of the DC field, H_o, and the RF field, H_1, has Y'-polarization. In (B) the c-axis makes arbitrary angle θ with the direction of H_o and the RF field is shown with Y'-polarization.

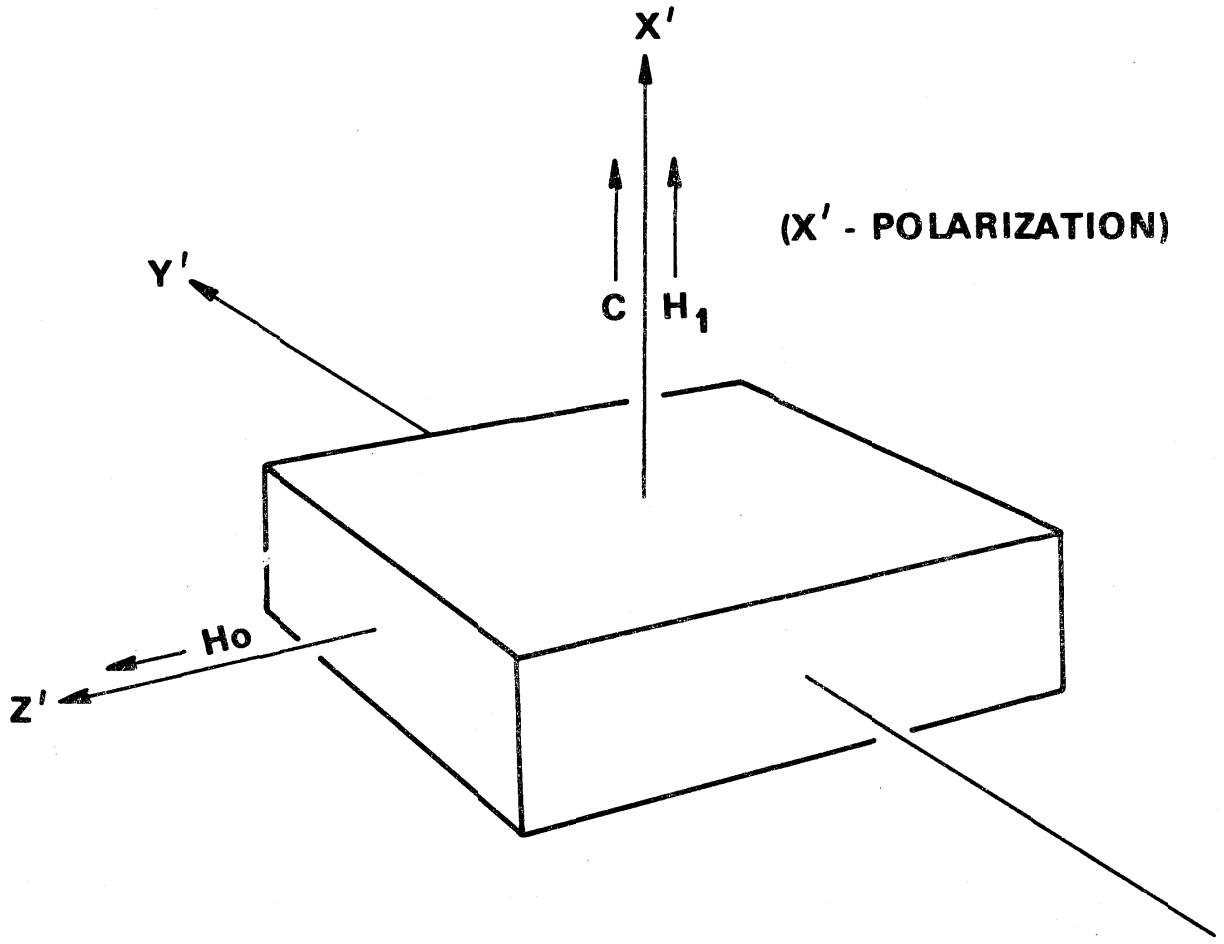

Fig. 14. Schematic drawings demonstrating the relative orientation of the wafer SRM and the laboratory coordinate system x'y'z'. The c-axis is perpendicular to the direction of the DC field, H_o. The RF field, H_1, has X'-polarization.

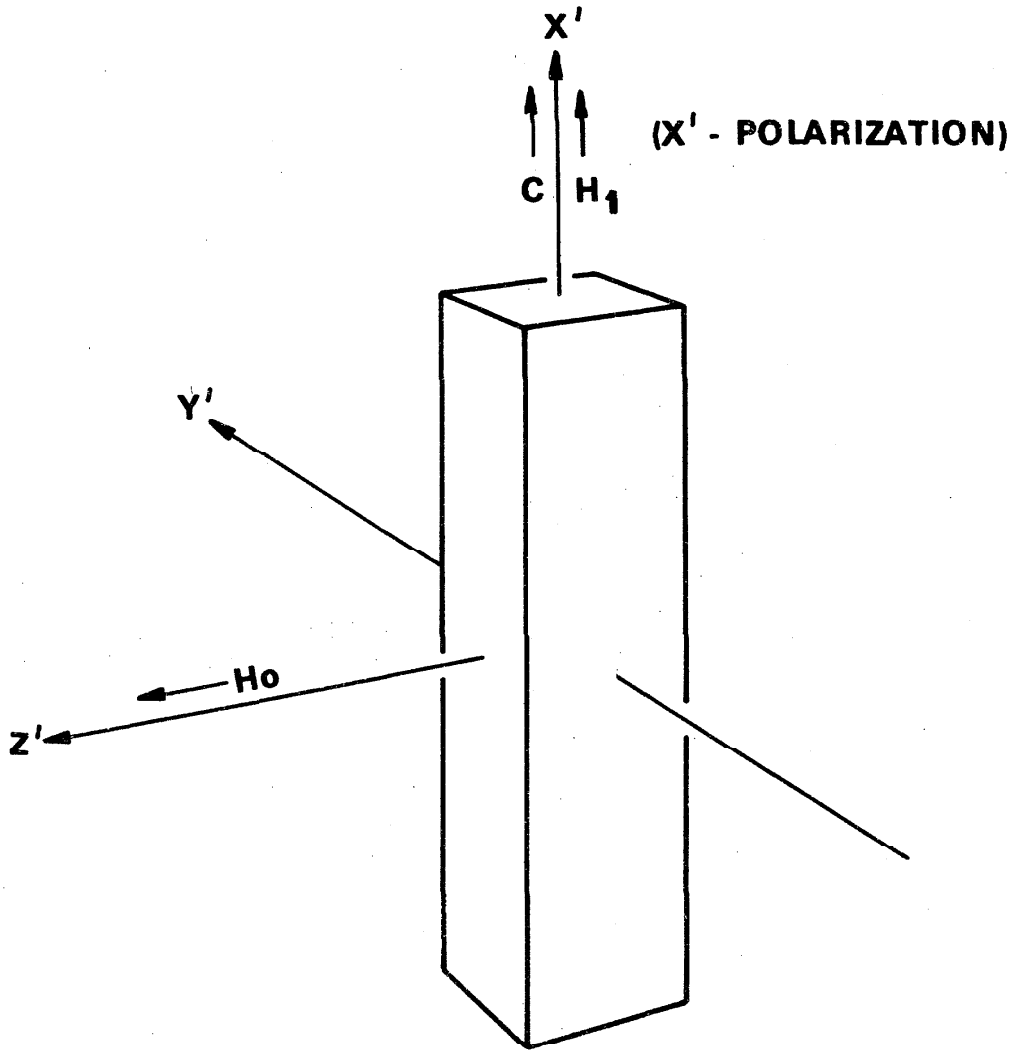

Fig. 15. Schematic drawings demonstrating the relative orientation of the bar SRM and the laboratory coordinate system x'y'z'. The RF field, H_1, has X'-polarization.

following, we follow the convention of the beginning of this chapter, that H_o is always horizontal and H_1 vertical.

In Figs. 12 through 15 we show two typical mountings of the ruby SRM specimens. In each case we show how H_o can be rotated with respect to the specimen. In two of the cases (Fig. 12 and Fig. 13) angle θ changes as the field H_o is rotated; in the other two cases (Fig. 14 and Fig. 15) θ is fixed at 90°. In each figure the appropriate polarization x'- or y'- is listed. When $\theta = 90°$ the sample may be rotated about the x' axis with no change in the spectrum or the intensity. It is important for the user to be familiar with the mode of the cavity he is using and to understand the correspondence of the illustrated fields and crystal orientations to his own laboratory configurations. If the orientation of the c-axis is not correctly ascertained, the resonance field will not agree with the tabulated values. If the wrong polarization is presumed, the intensity also will not agree with the tabulation.

4.4 Test Run with the Ruby SRM

The features of the Cr^{3+} EPR spectrum that have been described can be observed by a test run with either piece of the ruby SRM. With the aid of the graphs and the tabulated information supplied in this publication, the resonance transition should be readily locatable. It is advisable to start with the angular position of $\theta = 0°$. At 9.5 GHz, the (1/2,-1/2) transition is at 3425.0 Oe (see Fig. 16). A slight difference of the microwave frequency from 9.5 GHz, and slight miscalibration of the control setting of the magnetic field of the spectrometer may cause the transition to occur at shifted field readings. Slight misalignment from the $\theta = 0°$ condition will also displace the transition. This misalignment can be corrected by rotating the sample holder or the electromagnet with respect to each other. At 9.5 GHz, as seen from the angular dependence curve (see Fig. 2 and Table 2), the (1/2,-1/2) transition occurs at a maximum. Slight deviation from the $\theta = 0°$ condition will cause both the resonance magnetic field and the line intensity to decrease. Hence, by varying the angular setting the $\theta = 0°$ position can be located by maximizing the field value and the intensity of the (1/2,-1/2) transition. This transition should have a line width of about 15 Oe between points of steepest slope. The two outer halves of the two outer hyperfine lines should be clearly resolved at room temperature. For the (3/2,1/2) transition, the two outer halves appear as two extended wings. At 359.4, 1141.8 and 3784.4 Oe, the positions of forbidden transitions, no signal should be observed. If θ is set to 90°, the spectrum will consist of two transitions occurring at 1953 and 5387 Oe. The intensity ratio of these two transitions will unambiguously verify the assignment of the polarization of the microwave field. (See Sec. 2.4, 4.3, and 5.2.2.)

For other frequencies, of course, the transitions occur at different fields, but the same principle to locate the c-axis as just described still applies. The verification of the polarization of the microwave field may have to be more carefully done.

One should become familiar with the Cr^{3+} EPR spectrum before putting the SRM into practical use.

5. Measurement of the Number of Spins

5.1 The Area under the Absorption Curve

The area under the absorption curve can be obtained by digital computer or by hand calculation. The usual procedure is to sweep the static field, H_o, through values from H_a to H_b, where the interval from H_a to H_b contains the entire resonance line being measured. The signal, S(H), obtained, which is proportional to the derivative of the absorption curve, is recorded for n equally spaced values of H_o. We enumerate the field values as H_a, H_2, H_3..., H_{n-1}, H_b; and the corresponding measured values of S(H) as $S(H_a)$, $S(H_2)$, $S(H_3)$ ..., $S(H_{n-1})$, $S(H_b)$. The units of H are in oersteds and the units of S(H) are arbitrary and depend on the sensitivity and gain of the spectrometer. It is assumed that the scan range, H_a to H_b, completely encloses the line, so that S(H) vanishes near each end of the interval.

The area, A, is defined by the double integration of the derivative signal as follows:

$$A = \int_{H_a}^{H_b} dH \int_{H_a}^{H} dH' \, S(H') \quad . \tag{8}$$

In computer controlled EPR instruments there is usually a provision for calculating this integral numerically, the evaluation involves calculation of A by the procedure:

$$\begin{aligned} A \simeq \left[\frac{H_b - H_a}{n-1}\right]^2 [& S(H_a) \\ & + S(H_a) + S(H_2) \\ & + S(H_a) + S(H_2) + S(H_3) \\ & + \ldots \\ & + \ldots \\ & + S(H_a) + S(H_2) + S(H_3) + \ldots + S(H_b)] \quad . \end{aligned} \tag{9}$$

If the EPR spectrometer has no computer associated with it, S(H) can be recorded by a strip chart recorder and digitized by hand. The integration of Eq. (9) can then be performed by hand. (See Fig. 16.)

Consecutive measurements with both samples placed in the cavity together is preferable to successive substitution of the samples. If the scan ranges, H_b-H_a, or the number of points, n, are different for the two resonances, the user must take care to see that the proper calculation of Eq. (9) is carried out. Users of manufacturer-supplied computer programs for spin concentration should be sure that changes in these quantities are given appropriate accounting. Proper adjustment of the zero line and correction for base line drift should be incorporated in the integration process [4,7].

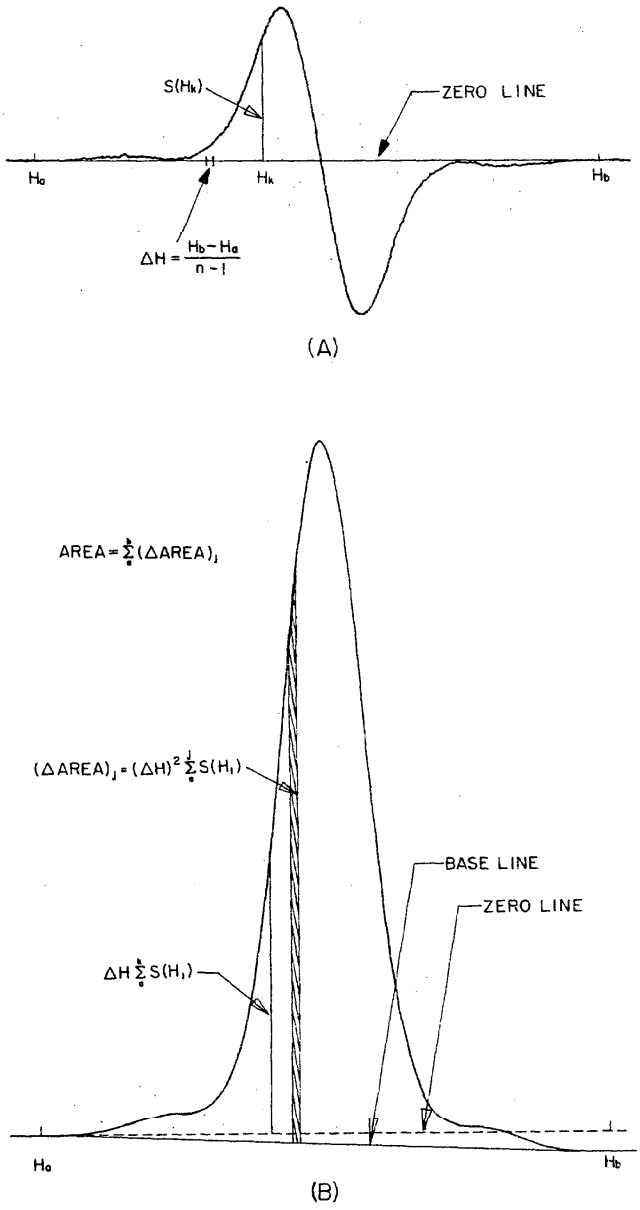

Fig. 16. Paramagnetic resonance absorption of Cr^{3+}, (1/2,-1/2) transition, with H_o parallel to the c-axis of the ruby crystal. In (A) the observed signal, the derivative of the absorption profile vs. applied field H_o, as obtained from the spectrometer is shown. The scan range H_b-H_a is 95 Oe. In (B) the absorption signal vs. applied field H_o is shown, as obtained from (A) by a single integration. Ordinate is in arbitrary units.

5.2 The Comparison of Integrated Areas of Two EPR Lines

By evaluating the ratio of the areas of two EPR lines it is often possible to determine the ratio of the number of spins which give rise to the two lines. The ratio of the two areas, A_1 and A_2, from Eq. (4), can be written as the product of four ratios, as follows:

$$\frac{A_1}{A_2} = \frac{\text{Spect. Gain}_1}{\text{Spect. Gain}_2} \times \frac{\langle H_1^2 \rangle_{s_1}}{\langle H_1^2 \rangle_{s_2}} \times \frac{\text{Integr. Intensity}_1}{\text{Integr. Intensity}_2} \times \frac{N_1}{N_2} \qquad (10)$$

If the ratio A_1/A_2 is measured and if the first three factors of the righthand side of Eq. (10) are known, then the ratio N_1/N_2 can be found.

The first factor, the ratio of spectrometer gain factors of the two resonances can be set equal to unity if the spectrometer conditions are the same for the two resonances. If not, this factor can be measured.

The second factor will be unity if both resonances come from the same value of RF field H_1. This would be the case if two small samples are used and they are placed in the cavity adjacent to each other. If the two samples are placed at different sites in the cavity, or if they are extended, it will be necessary to know the ratio

$$\langle H_1^2 \rangle_{s_1} / \langle H_1^2 \rangle_{s_2}.$$

This can be obtained from calculated filling factors [3] or by mapping the H_1 field in the cavity (see Appendix 2).

The third factor is the ratio of the integrated intensities per spin. The integrated intensity per spin for a general transition (α,β) is given by the quantity [7]

$$\left[\begin{array}{l}\text{Integrated Intensity for} \\ \text{a general transition}\end{array}\right] = \frac{\pi^2 g^2 \mu_B^2 \nu^2}{(2S+1)\ kT} \frac{|\langle \alpha | S_\ell | \beta \rangle|^2}{\left|\frac{d\nu_{\alpha\beta}}{dH_o}\right|} , \qquad (11)$$

where S_ℓ is the component of the spin angular momentum, S, along H_1 and $(d\nu_{\alpha\beta}/dH_o)$ is the weighting factor for the transition. For Cr^{3+} in ruby this factor may be put in the convenient form

$$\left[\begin{array}{l}\text{Integrated Intensity} \\ \text{for ruby}\end{array}\right] = \frac{\pi^2 g \nu^2 h \mu_B}{4kT} U_\ell^{\alpha,\beta} \qquad (12)$$

where $U_{\ell}^{\alpha,\beta} = \dfrac{|\langle\alpha|S_{\ell}|\beta\rangle|^2}{\left|\dfrac{d\nu_{\alpha,\beta}}{dH_o}\right|} \dfrac{g_{\parallel}\mu_B}{h}$ and is obtainable from Table 1 through Table 7.

Details of the passage from Eq. 11 to Eq. 12 may be found in Ref. 7. The integrated intensity for the unknown sample must be determined for each particular case. Several examples are given in the next part of this section.

5.2.1 Use of the ruby SRM with H_o parallel to the c-axis; test sample with spin 1/2. The simplest use of the ruby SRM for intensity comparison occurs when the ruby is oriented with the c-axis parallel to the static field, H_o. If the test sample has spins with the value S = 1/2 and an isotropic g-factor (e.g., DPPH), a very simple measurement of the number of spins is possible. We assume that the test sample and the SRM experience the same values of RF field amplitude. We compare the area of the test sample resonance with the area of the (1/2,-1/2) resonance of the SRM. From the preceeding discussion and Ref. 7, the ratio of the areas is

$$\frac{A}{A_o} = \frac{1}{2}\frac{N}{N_c}\frac{g}{g_o} \quad , \tag{13}$$

where the N's are the total numbers of spins, and the g's are the spectroscopic splitting factors; unsubscripted symbols pertain to the test sample and zero-subscripted pertain to the standard sample. In this case, the tables are needed only to locate the field for the (1/2,-1/2) transition of the ruby.

If the (3/2,1/2) transition of the SRM is used, the area ratio becomes

$$\frac{A}{A_o} = \frac{1}{1.5}\frac{N}{N_o}\frac{g}{g_o} \tag{14}$$

If the test sample has spin higher than 1/2 the discussion of the general case, Sec. 5.2.4, should be applied.

The principal objection to using the ruby SRM with H_o parallel to the c-axis is that the ruby resonance of the (1/2,-1/2) transition occurs at static fields in the g = 2 region. Thus, in many cases the EPR lines of the test sample and the standard sample will interfere with each other. This difficulty can be avoided by using the ruby SRM in a different orientation.

5.2.2 Use of the ruby SRM with H_o perpendicular to the c-axis; test sample with spin 1/2. For x-band radiation (9.5 GHz) the EPR spectrum of ruby consists of two lines at 1954 Oe and 5387 Oe. Between these two

field values is a large "window" in which most commonly occurring resonances can be observed. Hence, this orientation offers convenient use. In addition, the resonance fields and integrated intensities of the ruby SRM lines, in the vicinity of $\theta = 90°$, vary slowly with angle so that alignment is not critical.

If again, the test sample has spin 1/2 and an isotropic g-factor, and the RF field amplitudes are the same at the test and standard sample sites, the ratio of the areas is

$$\frac{A}{A_o} = \frac{1}{2}\frac{N}{N_o}\frac{g}{g_o}\frac{1}{U^{\alpha_o\beta_o}} \quad , \tag{15}$$

where the symbols A, N, and g are the same as before, and the factor $U^{\alpha_o\beta_o}$ is the normalized integrated intensity given in Table 1 through Table 7. One finds the value of $U^{\alpha_o\beta_o}$ by identifying the transition (α_o,β_o) observed and the polarization of the RF field.

We offer an example as a demonstration. Let the resonance frequency be 9.5 GHz and let y'-polarization be used. Assume we have decided to use the resonance at 5387 Oe as the standard resonance. Then from Table 2 we find that at angle $\theta = 90°$, the appropriate U factor is

$$U_{y'}^{3,4} = 0.470 \quad . \tag{16}$$

For this case, the ratio of areas is

$$\frac{A}{A_o} = \frac{N}{N_o}\frac{g}{g_o}\frac{1}{0.940} \quad . \tag{17}$$

The value of g_o is 1.9818.

The 90° orientation has a convenient safeguard for checking that the polarization is correctly identified. If the polarization is of the y'-type, the resonance at field 1954 Oe should have approximately twice the integrated intensity of the resonance at 5387 Oe, as is seen from the U-factors of Table 2, $\theta = 90°$. If the polarization is of x'-type the resonance at 1954 Oe should have approximately one-fourth the integrated intensity of the resonance at 5387 Oe. The difference in these ratios is so pronounced that the polarization type (x'- or y'-) is unambiguously verified from the observed signals by inspection.

5.2.3 Arbitrary orientation of the ruby SRM; test sample with spin 1/2. Eq. (15) of the previous section can be generalized to the case of arbitrary orientation of the ruby SRM with respect to the static field. For the case of a test sample with S = 1/2 and an isotropic g-factor, Eq. (15) applies directly. However, one must use the value of U for the angle θ used, and for the appropriate transition and RF polarization. The user must provide a means of measuring the angle between the c-axis

and the static field, H_o. If an angle other than a multiple of 10° is desired, graphical interpolation of the resonance fields and U-factors is satisfactory.

5.2.4 Arbitrary orientation of the ruby SRM; test sample of arbitrary spin. If one of the resonance lines is from the ruby SRM the ratio of intensities becomes

$$\frac{A}{A_o} = \frac{\frac{Ng^2}{2S+1} |\langle\alpha|S_\ell|\beta\rangle|^2 \frac{1}{|d\nu_{\alpha\beta}/dH|}}{\frac{N_o g_o h}{4\mu_B} U^{\alpha_o\beta_o}(\theta)} \qquad (18)$$

where zero subscripts refer to the standard resonance ($\alpha_o\beta_o$) and U is the appropriate normalized integrated intensity found in Table 1 through Table 7. The user must know the spin Hamiltonian of the test sample in order to evaluate the matrix element and the weighting factor. If the resonance spectrum shows fine structure, angular dependence, or both, the spin Hamiltonian must be examined if a concentration measurement is to be made.

5.3 Calibration and Use of a Working Standard

In some applications it may not be desirable to use the ruby SRM and a secondary working standard may be needed. This might occur, for example, in cases where intense UV radiation is present and the ruby fluorescence would interfere with the experiment. The working standard can be of any material that has a suitable EPR signal.

If a working standard is needed, it should be calibrated against the ruby. The following discussion offers a procedure for the calibration. As an example, we consider the TE_{102} rectangular cavity, as illustrated in Fig. 9. The working standard might be located on the cavity wall. (Any location which will produce a good resonance is satisfactory.) Before performing measurements on the test sample, a ruby SRM should be positioned at the test sample site and the intensity of the working standard compared with that of one of the transitions of the ruby. From this comparison one can then transfer the intensity measurement from the ruby standard to the working standard.

5.4 Use at Other Than Room Temperature

The EPR signal from Cr^{3+} in ruby can be observed from the lowest temperatures attainable (below 1 °K) to above room temperature. Specially designed cavities are needed at extreme temperatures. At low temperatures saturation [3] of the EPR resonance may be troublesome. Power levels should be kept low enough to avoid saturation. At high temperatures the line shape and line width will change.

5.5 Precautions Concerning Visible, UV, X-Ray and Nuclear Radiations

It is well known that ruby suffers damage from intense radiation [8]. Usually nuclear radiations are not encountered in EPR experiments. However, it is possible that x-ray, UV, or strong visible light may be used in certain applications. This may cause damage or may induce undesirable fluorescence.

Damage to ruby can be detected by a change of color, from pink to orange. This can be best observed against a dark background, preferably by comparison with an undamaged ruby SRM. Exposure to room light at room temperature for several days will usually bleach the discoloration. The effects of low levels of irradiation on the EPR signal is small and reversible [8].

In optical EPR experiments using UV irradiation, the ruby will usually fluoresce, giving off the prominent R-lines (at 694 nM). Some of the common varnishes or household cements used to attach the SRM to the cavity or holder, also fluoresce when excited by UV radiation. Precautions should be taken if this could interfere with the planned experiment.

List of Symbols

A - Area under resonance absorption curve in arbitrary units.

D - Axial crystal field splitting parameter.

E_m - Energy level belonging to state specified by m.

ΔE - Energy spacing between levels.

$g_{\parallel}$, $g_{\perp}$ - Spectroscopic splitting factors.

h - Planck's constant.

H_o - DC magnetic field.

H_1 - RF magnetic field.

k - Boltzmann's constant.

m - Azimuthal quantum number.

n - Number of equally spaced field points for digitizing the absorption curve.

N - Total number of spins in a sample.

S - Spin quantum number.

S_ℓ - Component of spin operator along the direction of H_1.

S(H) - Experimentally observed signal, proportional to the derivative of the absorption curve at field H_o.

T - Absolute temperature.

$T_{x'}$, $T_{y'}$ - Transition probability rates for polarization x' or y'.

$U_{x'}$, $U_{y'}$ - Field sweep integrated intensity per spin, for polarization x' or y'.

V_c - Volume of microwave cavity.

V_s - Volume of sample.

(α,β) - Specification of transition between states symbolized by α and β.

η - Filling factor.

μ_B - Bohr magneton.

ν - Frequency of microwave radiation.

$\nu_{\alpha\beta}$ - $(E_\alpha - E_\beta)/h$, the frequency corresponding to the energy difference between levels α and β.

REFERENCES

1. C. P. Slichter, Principles of Magnetic Resonance (Harper and Row, New York, 1963).

2. C. P. Poole, Jr. and H. A. Farach, The Theory of Magnetic Resonance (John Wiley & Sons, Inc., New York, 1972).

3. C. P. Poole, Jr., Electron Spin Resonance (Interscience Publishers, New York, 1967).

4. R. S. Alger, Electron Paramagnetic Resonance (Interscience Publishers, New York, 1968).

5. A. Abragam and B. Bleaney, Electron Paramagnetic Resonance of Transition Ions (Clarendon Press, Oxford, 1970).

6. D.J.E. Ingram, Biological and Biochemical Applications of Electron Spin Resonance (Plenum Press, New York, 1969).

7. T. Chang, D. Foster, and A. H. Kahn, J. Res. Natl. Bur. Standards (U.S.) 83, 133 (1978).

8. R. F. Wenzel, J. J. Halpin, and F. J. Campbell, Report NRL-7063 (AD-704069), Naval Res. Lab., Washington, D. C. (20 Feb. 1970).

Appendix 1. MAGNETIC FIELD UNITS

A short explanation of the units used in this publication follows. The energy of an atomic magnetic moment in an applied magnetic field is determined by the magnetic field strength, H. The most commonly used unit of H in the practice of magnetic resonance is the c.g.s. electromagnetic unit, the oersted, abbreviated Oe. Accordingly, we use the oersted in this report. The magnetic induction, B, is measured in the c.g.s. electromagnetic system in gauss, abbreviated G. For this system of units, in vacuum B has a numerical value equal to the value of the field strength, H, and the two are sometimes referred to interchangeably. The SI (Systeme International) unit of H is the ampere/meter (A/m) and that of B is the tesla (T). The quantities H and B may be converted from c.g.s. electromagnetic units to SI units by the formulas:

$$H(A/m) = H(Oe) \times 10^{3}/4\pi$$

$$B(T) = B(G) \times 10^{-4}.$$

Appendix 2. USE OF THE RUBY SRM WITH A LARGE TEST SAMPLE

We expect that many users will want to determine the number of spins in a sample which is so large that the RF field will not be uniform over the spatial extent of the sample. This may occur when a long flat quartz cell is used to hold a liquid sample. In this case it is necessary to find the change of signal strength arising from the non-uniformity of the RF field amplitude.

We shall illustrate the method of accounting for the variation of field amplitude by considering the use of a flat quartz cell for liquid samples. Both pieces of the ruby SRM, will be used. One piece is placed at a fixed position in the cavity and is used as a reference for measuring the average H_1^2 in the sample cell. The second piece is mounted on the flat quartz cell and can be moved over the region of the cavity to be occupied by the experimental sample. The two pieces should be so arranged that the resonance signals from both pieces can be observed simultaneously. When the movable piece is at the center of the cavity its signal will be a maximum. When it is moved away from the center, the field H_1 will be reduced and the signal will be weaker. By measuring the signal strength at several positions along the region where the experimental sample will reside, one can obtain an average of the signal strength. The ratio of the averaged signal to the maximum signal (with the SRM at the center of the cavity) is equal to the ratio of the average of H_1^2 to the value at the maximum.

During measurements on test samples, the SRM fixed to the quartz cell can be used as a standard for comparison with the unknown. The intensity of the resonance of the test sample should be multiplied by the factor

$$(H_1^2)_{maximum} / (H_1^2)_{average}$$

to correct for the fact that portions of the extended test sample see a smaller field than the maximum.